

SANDIA REPORT

SAND2010-7141

Unlimited Release

Printed September 2010

Development of Efficient, Integrated Cellulosic Biorefineries

LDRD Final Report

Christopher R. Shaddix, Ethan Hecht, Kwee- Yan Teh, George Buffleben, Dean Dibble,
and Andrew E. Lutz

Prepared by

Sandia National Laboratories

Albuquerque, New Mexico 87185 and Livermore, California 94550

Sandia National Laboratories is a multi-program laboratory managed and operated by

Sandia Corporation, a wholly owned subsidiary of Lockheed Martin Corporation, for the U.S.

Department of Energy's National Nuclear Security Administration under contract DE-AC04-94AL85000.



Sandia National Laboratories

Issued by Sandia National Laboratories, operated for the United States Department of Energy by Sandia Corporation.

NOTICE: This report was prepared as an account of work sponsored by an agency of the United States Government. Neither the United States Government, nor any agency thereof, nor any of their employees, nor any of their contractors, subcontractors, or their employees, make any warranty, express or implied, or assume any legal liability or responsibility for the accuracy, completeness, or usefulness of any information, apparatus, product, or process disclosed, or represent that its use would not infringe privately owned rights. Reference herein to any specific commercial product, process, or service by trade name, trademark, manufacturer, or otherwise, does not necessarily constitute or imply its endorsement, recommendation, or favoring by the United States Government, any agency thereof, or any of their contractors or subcontractors. The views and opinions expressed herein do not necessarily state or reflect those of the United States Government, any agency thereof, or any of their contractors.

Printed in the United States of America. This report has been reproduced directly from the best available copy.

Available to DOE and DOE contractors from

U.S. Department of Energy
Office of Scientific and Technical Information
P.O. Box 62
Oak Ridge, TN 37831

Telephone: (865)576-8401

Facsimile: (865)576-5728

E-Mail: reports@adonis.osti.gov

Online ordering: <http://www.doe.gov/bridge>

Available to the public from

U.S. Department of Commerce
National Technical Information Service
5285 Port Royal Rd
Springfield, VA 22161

Telephone: (800)553-6847

Facsimile: (703)605-6900

E-Mail: orders@ntis.fedworld.gov

Online order: <http://www.ntis.gov/help/ordermethods.asp?loc=7-4-0#online>



DEVELOPMENT OF EFFICIENT, INTEGRATED CELLULOSIC BIOREFINERIES

LDRD Final Report

Christopher R. Shaddix, Ethan Hecht, Kwee-Yan Teh,
George Buffleben, Dean Dibble, and Andrew E. Lutz

Sandia National Laboratories
Livermore, CA 94550

Abstract

Cellulosic ethanol, generated from lignocellulosic biomass sources such as grasses and trees, is a promising alternative to conventional starch- and sugar-based ethanol production in terms of potential production quantities, CO₂ impact, and economic competitiveness. In addition, cellulosic ethanol can be generated (at least in principle) without competing with food production. However, approximately 1/3 of the lignocellulosic biomass material (including all of the lignin) cannot be converted to ethanol through biochemical means and must be extracted at some point in the biochemical process. In this project we gathered basic information on the prospects for utilizing this lignin residue material in thermochemical conversion processes to improve the overall energy efficiency or liquid fuel production capacity of cellulosic biorefineries. Two existing pretreatment approaches, soaking in aqueous ammonia (SAA) and the Arkenol (strong sulfuric acid) process, were implemented at Sandia and used to generate suitable quantities of residue material from corn stover and eucalyptus feedstocks for subsequent thermochemical research. A third, novel technique, using ionic liquids (IL) was investigated by Sandia researchers at the Joint Bioenergy Institute (JBEI), but was not successful in isolating sufficient lignin residue. Additional residue material for thermochemical research was supplied from the dilute-acid simultaneous saccharification/fermentation (SSF) pilot-scale process at the National Renewable Energy Laboratory (NREL). The high-temperature volatiles yields of the different residues were measured, as were the char combustion reactivities. The residue chars showed slightly lower reactivity than raw biomass char, except for the SSF residue, which had substantially lower reactivity. Exergy analysis was applied to the NREL standard process design model for thermochemical ethanol production and from a prototypical dedicated biochemical process, with process data supplied by a recent report from the National Research Council (NRC). The thermochemical system analysis revealed that most of the system inefficiency is associated with the gasification process and subsequent tar reforming step. For the biochemical process, the steam generation from residue combustion, providing the requisite heating for the conventional pretreatment and alcohol distillation processes, was shown to dominate the exergy loss. An overall energy balance with different potential distillation energy requirements shows that as much as 30% of the biomass energy content may be available in the future as a feedstock for thermochemical production of liquid fuels.

This page left intentionally blank.

Table of Contents

Page

Abstract.....	3
Table of Contents.....	5
List of Figures.....	6
List of Tables.....	9
Acknowledgments.....	10
Introduction.....	11
Project Structure.....	11
Biomass Feedstocks and Pretreatment Strategies.....	13
Ionic Liquid (IL) Pretreatment.....	14
Soaking in Aqueous Ammonia (SAA) Pretreatment.....	16
Arkenol Pretreatment.....	17
Dilute-Acid SSF Process Residue.....	18
Thermochemical Evaluation of Lignin Residues.....	19
Residue Processing and Feeding.....	19
Initial Combustion Characterization.....	21
Improved Combustion Characterization.....	22
System Analysis.....	27
Thermochemical Ethanol System.....	27
Biochemical Ethanol System.....	32
Baker's Yeast Fermentation.....	36
Conclusions.....	37
List of References.....	38
Appendix A: LDRD Project Presentations and Publications.....	41
Appendix B: Arkenol Pretreatment Process Steps.....	42

List of Figures

Page

Figure 1. Schematic of typical current design layout for a biochemical ethanol biorefinery.....	13
Figure 2. Schematic of a potential future design layout for an ethanol biorefinery with primarily biochemical conversion and gasification of lignin residues.....	13
Figure 3. Schematic of a potential future design layout for an ethanol biorefinery with primarily biochemical conversion and fast pyrolysis of lignin residues.	14
Figure 4. Fractionation yields and product compositions from IL processing of corn stover.....	16
Figure 5. Photographs of corn stover and ionic liquid, (top left), stover in solution in heated IL (top right), and glucan-rich product of fractionation, adjacent to raw stover (bottom).....	16
Figure 6. 2-D NMR spectra of aromatic entities in corn stover and in its IL-prepared fractions. The circles identify particular structural elements corresponding to guaiacyl (“G”) and p-coumarate (“PCA”) units, with particular structures indicated schematically. Syringyl structures (“S”) appear at the top of the spectra	17
Figure 7. Photographs of dried, chopped corn stover (left), dried solids remaining after SAA treatment of the corn stover (middle), and lignin residue collected by drying the ammonia effluent (right).....	18
Figure 8. Schematic of the Arkenol pretreatment process, as appeared in Yamada et al., 2002	19
Figure 9. Photographs of chopped eucalyptus (left) and processed solids remaining after a single hydrolysis step using 77% sulfuric acid	19
Figure 10. Photograph of custom-designed fine particle feeder for dry coal and biomass samples. For feeding of particularly sticky biomass samples, steel shot can be added to the test tube to help break-up particle aggregates	20
Figure 11. Schematic of the Sandia’s optical entrained flow reactor facility, with a Hencken burner providing a high-temperature, high flow furnace environment and a particle-sizing pyrometry diagnostic measuring the temperature, size, and velocity of individual reacting particles	21

Figure 12. Photograph of a devolatilizing stream of lignin residue produced by SAA pretreatment of corn stover. Furnace temperature of 1500 K.....	21
Figure 13. Photographs taken through a microscope of SAA-generated lignin residue from corn stover knife-milled and sieved into different size classes: (a) fines, < 37 μm , (b) 75-106 μm , (c) 106-180 μm	22
Figure 14. Photographs of 75-106 μm corn stover SAA lignin residue burning in a 1200 K furnace with 12%, 24%, 36%, and 60% O_2 , respectively	23
Figure 15. Photographs of 106-180 μm particles of different lignin residues burning in 36% O_2 in a 1700 K furnace. The leftmost two photos show two different corn stover SAA pretreatment residues and the rightmost photo shows a eucalyptus SAA process residue.....	23
Figure 16. Schematic of Sandia’s Pressure-Capable Entrained Flow Reactor (PCEFR).....	24
Figure 17. Photographs of combustion of chars generated from raw and Arkenol-pretreated eucalyptus and of direct combustion of residues from pretreated corn stover in the optical EFR at 1700 K. “%” labels refer to oxygen content of flow. “Arkenol-1” refers to single-step hydrolysis and “Arkenol-2” refers to dual-step hydrolysis	25
Figure 18. Mean corn stover residue char combustion particle temperatures measured as a function of height in Sandia’s optical EFR when operating at 1700 K.....	26
Figure 19. Mean eucalyptus residue char combustion particle temperatures measured as a function of height in Sandia’s optical EFR when operating at 1700 K.....	27
Figure 20. Mean corn stover residue char combustion particle temperatures measured as a function of height in Sandia’s optical EFR when operating at 1700 K.....	27
Figure 21. Simplified block flow diagram of NREL’s canonical thermochemical ethanol process design	29
Figure 22. Energy inputs and outputs (left pie chart) and exergy inputs and outputs (right pie chart) for the 2012 design case thermochemical ethanol process.....	29

Figure 23. (Left) The dual-bed, indirect steam gasifier model overlaid on the NREL process flow diagram. (Right) Gasifier system exergy inputs and outputs.....	30
Figure 24. Schematic of the modeled gasifier block system (left) and the calculated exergy loss of the system as a function of the excess air supplied to the char combustor (right).....	31
Figure 25. (Left) The alcohol synthesis reactor overlaid on the NREL process flow diagram. (Right) Synthesis reactor exergy inputs and outputs.....	31
Figure 26. Schematic of the modeled wood dryer block system (left) and the calculated exergy loss of the system as a function of the inlet air temperature (right).....	32
Figure 27. Exergy budget for the thermochemical ethanol design case using 2007 and 2008 “state of technology” performance assumptions and the target 2012 design case.....	33
Figure 28. Schematic of a prototypical lignocellulosic biochemical ethanol plant, utilizing separate enzymatic hydrolysis and fermentation steps.....	34
Figure 29. Energy inputs and outputs (left pie chart) and exergy inputs and outputs (right pie chart) for the “low-performance” biochemical process design case.....	34
Figure 30. Exergy budget for the prototypical biochemical conversion process based on NRC technology performance scenarios.....	35
Figure 31. Energy consumption for ethanol distillation as a function of the ethanol in the feed to the distillation process and the technology employed (data from Madson and Lococo, 2000; Vane, 2008; Cote et al., 2008).....	36
Figure 32. Trade-off between electricity and thermochemical biofuel production using lignin-rich residue from a prototypical biochemical conversion process.....	36
Figure 33. Schematic of modeled system of continuous culture of baker’s yeast fermenting glucose under anaerobic, glucose-limited conditions.....	37
Figure 34. Exergetic efficiencies of fermentation process, as a function of the cellular ATP consumption.....	37

List of Tables

Page

Table 1. Assumptions for NRC Low-, Medium-, and High-Performance Processes32

Acknowledgments

Manfred Geier, a postdoctoral research associate, assisted with some of the experiments on lignin residue devolatilization and char combustion.

Introduction

This report documents the results of a Laboratory Directed Research and Development (LDRD) project with the aim of improving the design and performance of future biorefineries that convert lignocellulosic biomass sources into ethanol and specialty chemicals. Dwindling supplies of conventional oil and increasing concern over greenhouse gas emissions have motivated the search for renewable liquid fuels. Biomass-derived liquid fuels are promising candidates, particularly in the U.S., with its large capacity for generating biomass (Perlack et al., 2005). Currently, farm and ethanol subsidies and a guaranteed ethanol market have fostered the production of a large corn ethanol market. However, corn-based ethanol production engenders significant CO₂ production and has limited potential to offset U.S. oil consumption. Far greater production potential and improved reductions of CO₂ are possible when converting lignocellulosic biomass (grasses, trees, crop residues, etc.) into ethanol. This promising technology has seen substantial research investments for several years, primarily focused on purely biochemical processing of the biomass to yield ethanol and specialty chemicals and on purely thermochemical processing of the biomass to yield similar products. Indeed, the U.S. Department of Energy office that oversees most of this research, the Office of Biomass Programs (OBP), has divided its biomass conversion program into these two focal areas for a number of years.

One of the primary advantages of the biochemical conversion process is the ease of handling and feeding biomass feedstocks into the process (at the pretreatment stage) and the limited sensitivity to the biomass moisture level, because of the aqueous nature of the conversion process itself. For the thermochemical process, higher ethanol fuel yields are possible and the process shows low sensitivity to the type of biomass feedstock, because all of the biomass can be effectively gasified. Biochemical processing can typically only convert 60-70% of the biomass feedstock to sugars, for subsequent fermentation to ethanol, because of the existence of several components of the biomass, particularly lignin, protein, and extractives, that do not contain sugar polymers. At present, the limitations on ethanol yield of the dedicated biochemical process are not seen as particularly restrictive, because the pretreatment and ethanol distillation steps require a substantial quantity of steam, which can just be generated by burning all of the lignin-rich residue from the process, as indicated in Fig. 1. However, efforts are being made to improve the performance of the biochemical process, particularly to reduce the heat requirements of the pretreatment process (by operation at a lower temperature) and the distillation process (by incorporating membrane-based separation/distillation, for example). Progress in reducing the steam requirements of these processes will then “liberate” the energy content of the lignin residue for potential use in a thermochemical “bottoming cycle,” as suggested in the diagrams shown in Figures 2 and 3. The prospect for such hybrid biochemical/thermochemical ethanol biorefinery designs motivates the research conducted in this LDRD project.

Project Structure

This project combined an investigation of state-of-the-art biomass pretreatment technologies with assessments of the combustion and gasification potential of realistic lignin extracts. In addition, energy and exergy balances were computed for benchmark thermochemical and biochemical conversion processes, to illuminate those process components that have the most

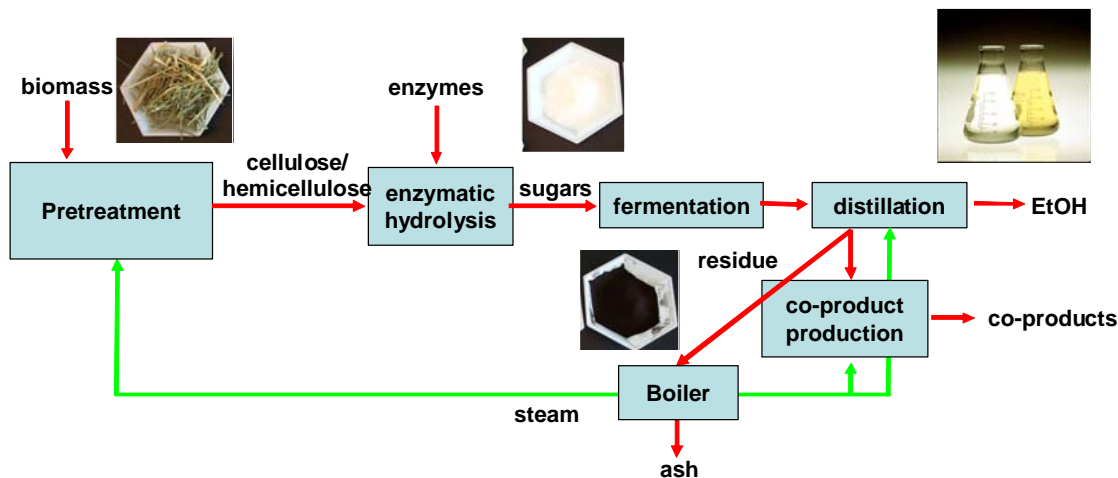


Figure 1. Schematic of typical current design layout for a biochemical ethanol biorefinery.

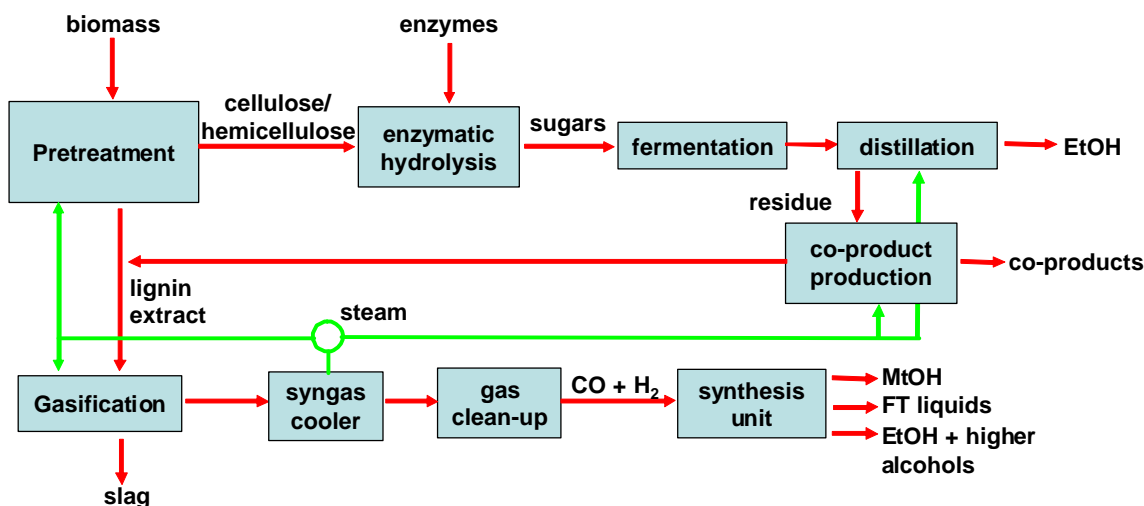


Figure 2. Schematic of a potential future design layout for an ethanol biorefinery with primarily biochemical conversion and gasification of lignin residues.

promise for yielding efficiency improvements. A particular focus of the project was on simple, low-cost pretreatment processes that directly separate lignin from the cellulose in the pretreatment step. These pretreatments have not been widely investigated, because from the point-of-view of a dedicated biochemical ethanol process, maximizing the conversion of both hemicellulose and cellulose to fermentable sugars is key to effective ethanol production. However, when considering hybrid biochemical/thermochemical ethanol biorefineries, a low-cost (and, especially, low-temperature) pretreatment process that extracts some hemicellulose with the lignin may be beneficial to the overall process efficiency and ethanol product yield in comparison to dilute acid pretreatment and other approaches that optimize biochemical

conversion of cellulose and hemicellulose. Information on the combustion, gasification, or pyrolysis behavior of lignin-rich residues from biochemical conversion processes is virtually non-existent in the literature (see Blunk and Jenkins, 2000; Eriksson et al., 2004; Öhman et al., 2006; and Li et al., 2008, for the only known examples), so work on this project should prove to be a vital source of information for designing appropriate thermochemical conversion devices.

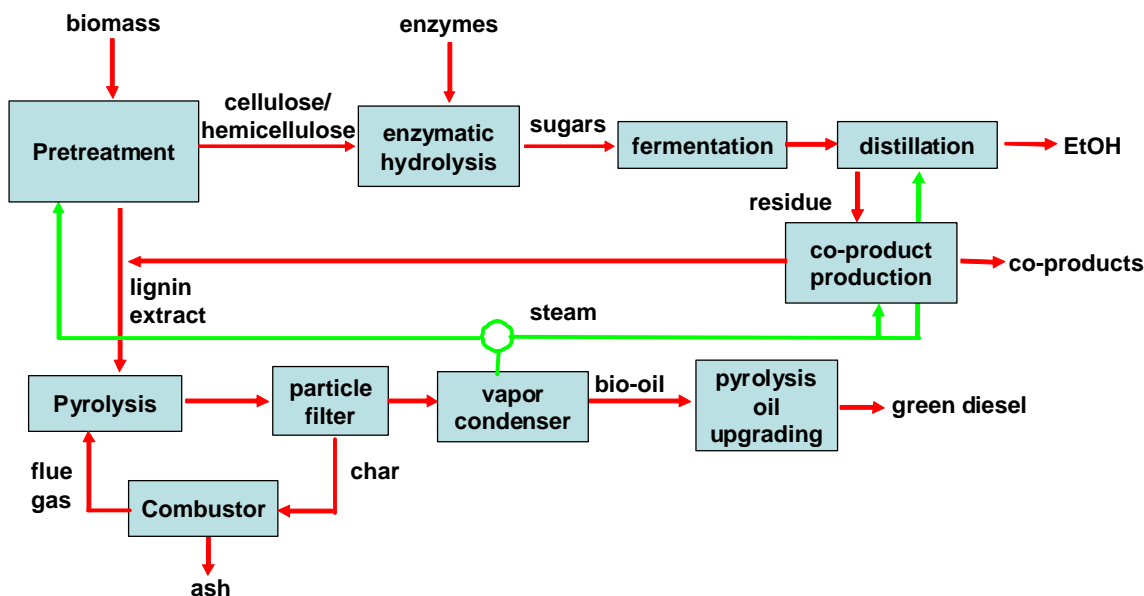


Figure 3. Schematic of a potential future design layout for an ethanol biorefinery with primarily biochemical conversion and fast pyrolysis of lignin residues.

Biomass Feedstocks and Pretreatment Strategies

A wide variety of biomass pretreatment approaches have been developed to augment the biochemical conversion of different biomass sources to ethanol (Kumar et al., 2009; Alvira et al., 2010). The general goals of biomass pretreatment for application to subsequent enzymatic hydrolysis are to increase the physical access to the cellulose and hemicellulose, to reduce the crystallinity of the cellulose, and to separate the lignin from the cellulose and hemicellulose (lignin blocks surface sites on the cellulose and hemicellulose from enzymatic attack). Different pretreatment approaches achieve these goals to different extents and with differing financial and energy costs. Acid-based pretreatment approaches chemically attack cellulose, whereas basic pretreatments directly attack the lignin. For this project, focus was given to implementing pretreatment approaches that would directly yield a lignin-rich residue, both because these approaches have not been widely investigated and because these approaches could most easily yield the 100's of g of residue that was required for subsequent thermochemical conversion analysis. The dilute sulfuric acid pretreatment, ammonia fiber expansion (AFEX) approach, and hydrothermal (steam expansion) approaches yield a residue at the end of the biochemical process and therefore were not investigated in this project. The three techniques that were implemented

and investigated during the course of this project included an ionic liquid (IL) approach, a technique known as “soaking in aqueous ammonia” (SAA), and the Arkenol process. The IL process research, which occurred at the Joint Bioenergy Institute (JBEI), was highly speculative and in the end did not yield sufficient usable lignin residue for subsequent thermochemical characterization. The other two approaches were implemented at the SNL/CA site and did yield substantial lignin residue that was subsequently investigated for thermochemical processing.

The biomass feedstocks that were utilized during this research were all derived from larger feedstock samples that were acquired for research at JBEI. These feedstocks included corn stover (a representative and widely investigated U.S. agricultural residue), switchgrass (a widely investigated herbaceous U.S. energy crop), and eucalyptus (a promising fast-growing softwood tree).

Ionic Liquid (IL) Pretreatment

In contrast to most proposed biomass pretreatment technologies, whose basic properties are reasonably well characterized, the ionic liquid pretreatment approach is a new and possibly revolutionary approach and thus has become the focus of pretreatment research at JBEI. The promise of ionic liquids is to eliminate the need for a separate pretreatment step and to rapidly hydrolyze the biomass polysaccharides (cellulose and hemicellulose) under mild conditions in which the depolymerization is highly selective (Sievers et al., 2009). Ionic liquids are essentially liquid-phase salts, and therefore retain a strong degree of dissociation into liquid-phase ions. This quality makes them powerful solvents. The first application of ionic liquids to dissolution of cellulose was reported in 2002 (Swatloski et al.), but this required a temperature of ~ 100 °C. Subsequent research developed ILs that can effectively dissolve cellulose at near room temperatures (Ohno and Fukaya, 2007). Dissolution of whole biomass is substantially more challenging than dissolution of cellulose, however, particularly because of the lignin component of lignocellulosic biomass. During the course of research into ionic liquid pretreatment as part of this project, a novel ionic liquid processing scheme for fractionating biomass was developed and has resulted in an expected patent filing (see Appendix). A couple of technical presentations have been made on this research (see Appendix) and a journal publication on the IL pretreatment has also been submitted (Dibble et al., 2010). Figure 4 shows a flow diagram that indicates the type of biomass fractionation that results from the IL process that has been developed. Fig. 5 shows photographs of ionic liquid treatment of corn stover and the glucan-rich product stream from this process.

Two-dimensional nuclear magnetic resonance (2-D NMR) imaging was performed at UC Berkeley on the different fractions produced by the IL processing as a way to track the disposition of lignin, per the technique reported by Kim et al. (2009, 2010). Fig. 6 shows the aromatic regions of the structure, indicative of lignin moieties. Particular structural entities are highlighted with circles and are defined below the figure. Similar NMR imaging has been conducted on both raw biomass and different pretreated samples, to compare the effects of pretreatment on the lignin bonding. This will be presented later in this report.

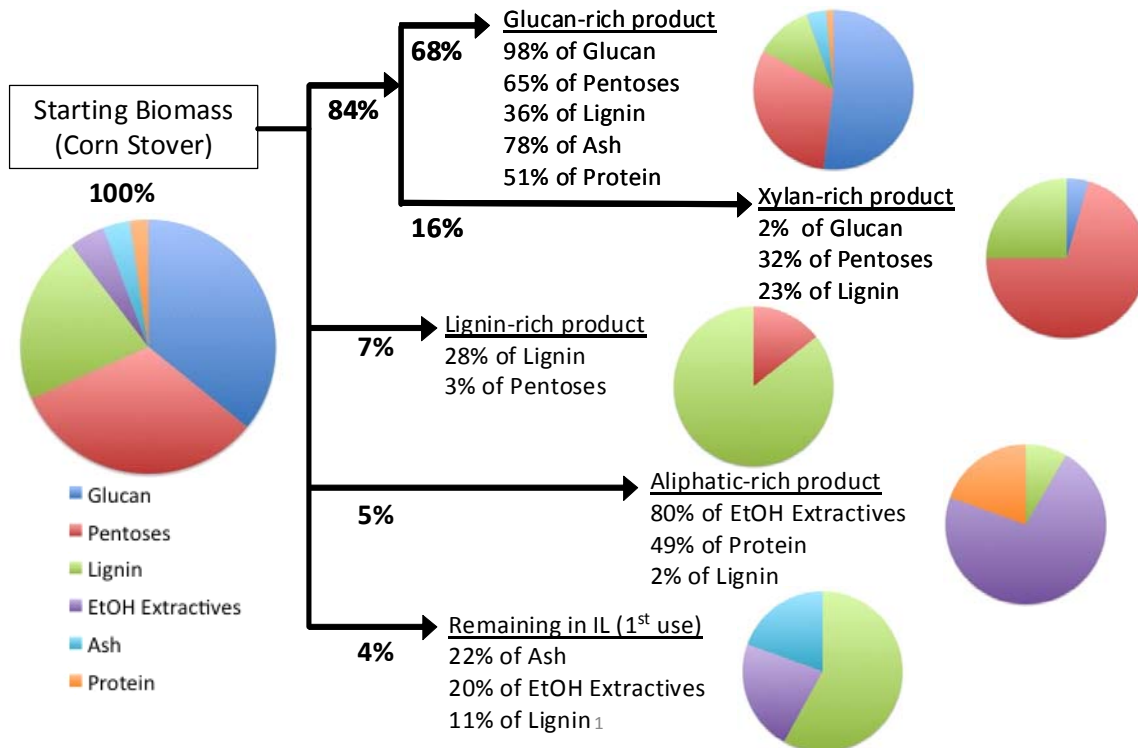


Figure 4. Fractionation yields and product compositions from IL processing of corn stover.

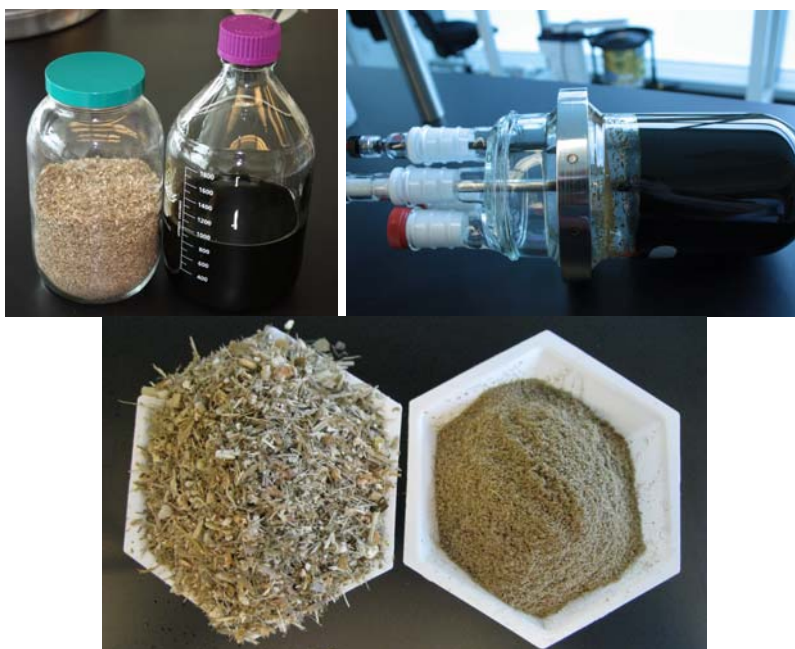


Figure 5. Photographs of corn stover and ionic liquid, (top left), stover in solution in heated IL (top right), and glucan-rich product of fractionation, adjacent to raw stover (bottom).

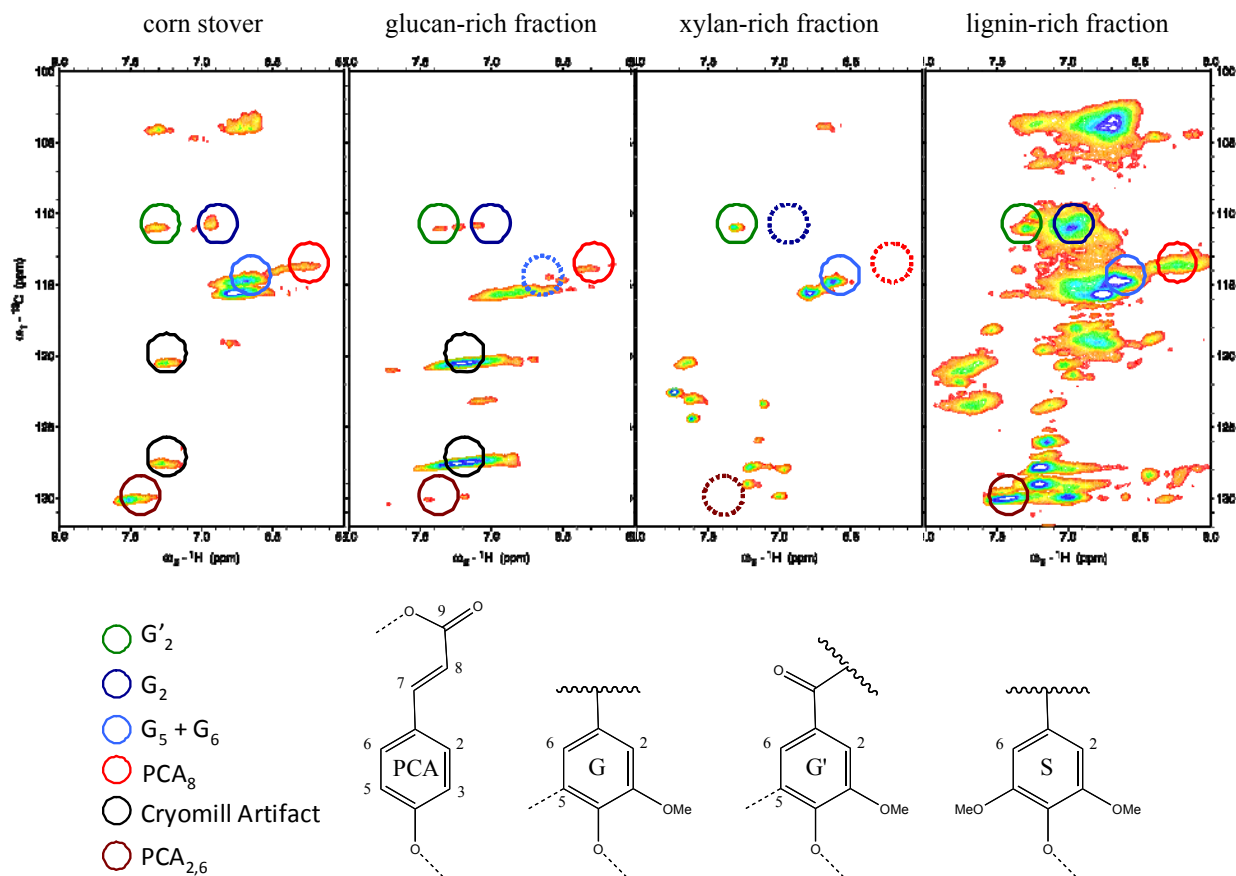


Figure 6. 2-D NMR spectra of aromatic entities in corn stover and in its IL-prepared fractions. The circles identify particular structural elements corresponding to guaiacyl (“G”) and p-coumarate (“PCA”) units, with particular structures indicated schematically. Syringyl structures (“S”) appear at the top of the spectra.

Soaking in Aqueous Ammonia (SAA) Pretreatment

A simple, low-energy pretreatment technique known as “soaking in aqueous ammonia” (SAA) that yields lignin residues directly from the pretreatment process was implemented, as this process is easy to scale-up to the sizable processing runs required to generate sufficient residues for thermal processing. This technique was developed by Prof. Yoon Lee of Auburn University (Yoon et al., 1995; Kim et al., 2003; Kim and Lee, 2005, 2007) and has been most recently applied by his former student, T.H. Kim (formerly of the USDA and currently at Iowa State University) (Kim et al., 2008; Li et al., 2010). Recently this technique was applied to the pilot-scale pretreatment of switchgrass in 4 kg increments in a 75 L vessel (Himmelsbach et al., 2009). In this process, the lignin is solubilized in the ammonia solution, together with a portion of the hemicellulose (linked C5 and C6 sugars). Subsequent drying of the solution yields a lignin residue. For optimized conditions with a 60 °C processing temperature, Kim and Lee (2007) report 62% lignin removal and 15% xylan removal from corn stover. Xylan removal was ~ 30% and lignin removal ~ 60% when applying SAA to barley hulls at 75°C (Kim et al., 2008). While

these removal fractions of hemicellulose make SAA somewhat disfavored for application in a dedicated biochemical biorefinery, wherein the solubilized hemicellulose is not available for subsequent fermentation to ethanol, this low-cost, low-energy pretreatment approach may prove to be advantageous in biorefineries that utilize integrated biochemical and thermochemical processing, wherein hemicellulose solubilization does not represent a conversion loss.

In this project, the moderate-temperature SAA process was refined and successfully applied to two different samples of corn stover (Midwest and California source material) and to eucalyptus wood. A 1:5 mixture ratio of dry biomass relative to 15% NH_4OH solution was used, and the mixture was heated to 60 °C and allowed to react for 37 hr. Chemical analysis of the solids derived from the SAA effluent from the two corn stover process treatments show that it is composed of ~ 50% lignin, with the remainder a mixture of hemicellulose sugars and inorganics. Fig. 7 shows photographs of the initial chopped corn stover feedstock, processed solids, and dried lignin residue (recovered from the ammonia wash).



Figure 7. Photographs of dried, chopped corn stover (left), dried solids remaining after SAA treatment of the corn stover (middle), and lignin residue collected by drying the ammonia effluent (right).

Arkenol Pretreatment

The Arkenol pretreatment process, which uses strong sulfuric acid to separate lignin from the cellulose and hemicellulose, was developed in the mid-1990's and was immediately patented (Farone and Cuzens, 1997, 1998; Cuzens and Miller, 1997). Currently, BlueFire Renewables owns the rights to the Arkenol process and is in the process of building commercial plants in Lancaster, CA, and in Fulton, MS, to produce ethanol from MSW and wood residues, respectively. A schematic of the Arkenol pretreatment process is shown in Fig. 8. In the strong acid process, the cellulose and hemicellulose are hydrolyzed and go into solution with the acid, leaving the lignin behind. Residual acid in the sugar solution is neutralized with lime, yielding solid gypsum as a byproduct. In this project, the Arkenol process was applied to the eucalyptus sample to provide a comparison with the residue derived from eucalyptus by applying the SAA process. The detailed procedure used for applying the Arkenol process is included as Appendix B. As a process summary, the raw biomass was reacted with 77% sulfuric acid and heated to 100 °C, then allowed to react for one hour. As shown in Fig. 8, in commercial applications the hydrolysis process is generally applied in two stages, where the second stage provides additional removal of the carbohydrates from the lignin. In this project, samples of the lignin residue from both one-step hydrolysis and two-step hydrolysis were produced for experiments on residue

thermochemical conversion. Fig. 9 shows photographs of the raw eucalyptus wood and the lignin-containing processed solids after a single hydrolysis step.

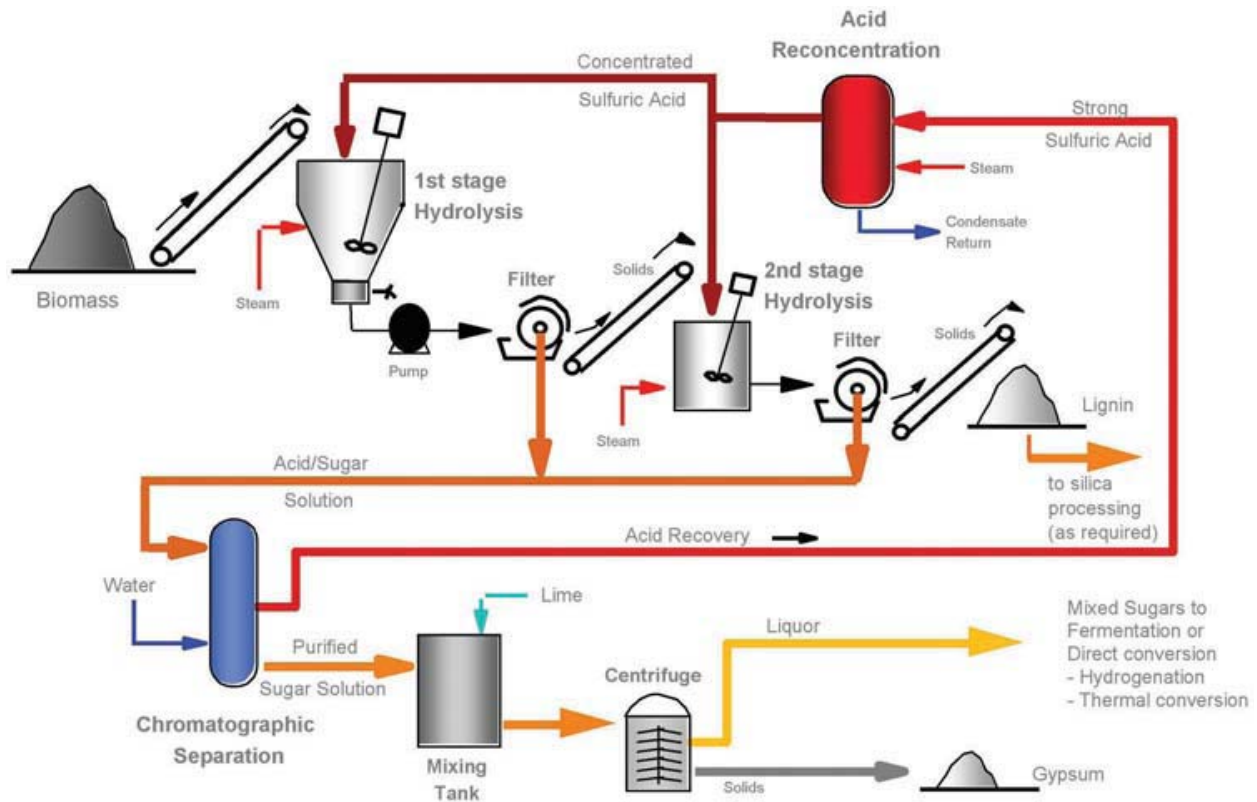


Figure 8. Schematic of the Arkenol pretreatment process, as appeared in Yamada et al., 2002.



Figure 9. Photographs of chopped eucalyptus (left) and processed solids remaining after a single hydrolysis step using 77% sulfuric acid.

Dilute-Acid SSF Process Residue

The most widely used lignocellulose pretreatment approach is undoubtedly dilute sulfuric acid pretreatment, which does not effectively hydrolyze the carbohydrates and therefore requires

subsequent enzymatic hydrolysis (e.g. as shown in Fig. 1), after neutralization and detoxification, to complete the hydrolysis of the polysaccharides (i.e. to complete “saccharification”). The National Renewable Energy Laboratory (NREL) has a pilot-plant configuration that has been investigating and optimizing dilute sulfuric acid pretreatment of corn stover followed by simultaneous saccharification and fermentation (SSF), a cost-reducing intensification of the process path. After distillation of the ethanol, the lignin-containing process dregs are removed. For this project, NREL researchers provided us with a sample of the lignin residue from their SSF process, when processing corn stover.

Thermochemical Evaluation of Lignin Residues

The goals of this portion of the project were to (a) evaluate methodologies for handling and feeding the lignin residues, because biomass particle feeding is generally an important practical consideration in both laboratory and commercial thermochemical processes, (b) evaluate the high-temperature, high-heating-rate volatiles content of the residues, because this is an important parameter in determining carbon conversion and minimum reactor size needed for combustion or gasification, and (c) measure the combustion/gasification reactivity of the residue char particles, for comparison to the existing experimental database of coals of various ranks.

Residue Processing and Feeding

The SAA corn stover lignin residues were dried and then initially were pulverized using an “Attritor” stirred-ball mill. This material was found to be feedable, with some plugging difficulties, in our new pulverized fuel feeder system for combustion analysis, shown in Fig. 10.



Figure 10. Photograph of custom -designed fine particle feeder for dry coal and biomass samples. For feeding of particularly sticky biomass samples, steel shot can be added to the test tube to help break-up particle aggregates.

With use of this feeder, high-temperature devolatilization experiments were conducted by operating our optical entrained flow reactor with a slightly fuel-rich fuel-oxidizer feed to the Hencken burner (see Figs. 11-12).

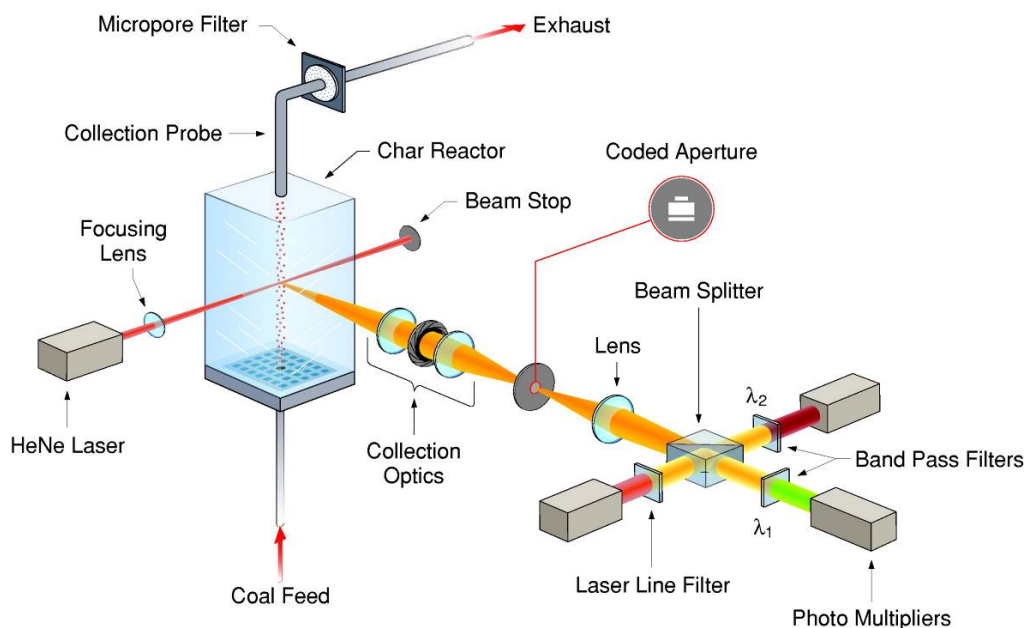


Figure 11. Schematic of the Sandia's optical entrained flow reactor facility, with a Hencken burner providing a high-temperature, high flow furnace environment and a particle-sizing pyrometry diagnostic measuring the temperature, size, and velocity of individual reacting particles.

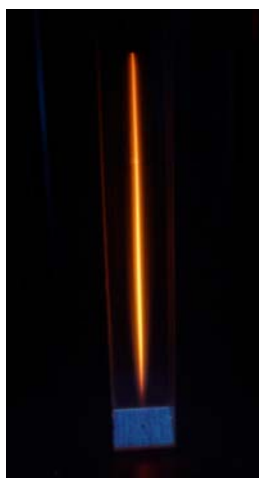


Figure 12. Photograph of a devolatilizing stream of lignin residue produced by SAA pretreatment of corn stover. Furnace temperature of 1500 K.

The particle size distribution of the residue processed with the Attritor was analyzed using an optical microscope, revealing that the overwhelming preponderance of particles were $< 10 \mu\text{m}$ in size and tended to form large particle agglomerates (i.e. the material behaved as fine dust). Both feeding and chemical kinetic analysis of combustion and gasification rates is improved for somewhat larger particles (on the order of $100\text{-}150 \mu\text{m}$ in size), so the lignin residues were resolidified and then milled with a Wiley knife mill, fitted with a custom-designed screen to provide an appropriately sized product output. The knife-milled residue was then sieved into three size classes and examined under a microscope, as shown in Fig. 13. The microscopy revealed that the particles were roughly spherical in shape (as opposed to the long fibrous particles generally produced from milling raw biomass) and segregated well in the sieving process.

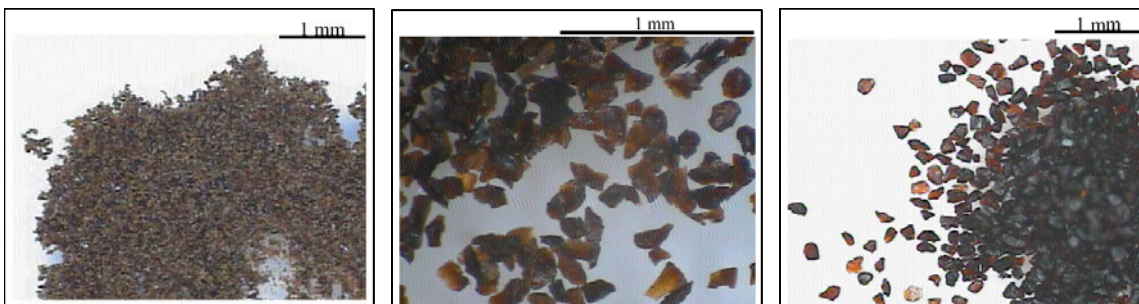


Figure 13. Photographs taken through a microscope of SAA-generated lignin residue from corn stover knife-milled and sieved into different size classes: (a) fines, $< 37 \mu\text{m}$, (b) $75\text{-}106 \mu\text{m}$, (c) $106\text{-}180 \mu\text{m}$.

Initial Combustion Characterization

Initial combustion experiments were performed at a low furnace temperature of 1200 K and oxygen concentrations of $12\text{-}60 \text{ vol-\%}$. Previous measurements in our laboratory have demonstrated that high oxygen concentrations in the flow are conducive to determination of the char combustion kinetic rates, because low oxygen concentrations can lead to oxygen diffusive control of the particle burning rate (Murphy and Shaddix, 2006). Lignin residue particles in the $75\text{-}106 \mu\text{m}$ size class were used for these experiments, because this particle size class has proven to be the optimal size for determination of the char combustion kinetics of coal. Fig. 14 shows time-lapse photographs of the lignin particles burning in the furnace at different oxygen concentrations. As the oxygen concentration increases, the particles appear to burn hotter (as denoted by the color of the visible emission from the particles) and burn out more quickly (as evidenced by the length of the visible particle streaks). In addition, the particles ignite earlier for a higher oxygen content of the flow. Attempts at performing single-particle particle-sizing pyrometry on the lignin residue particles proved difficult, because the particles would ignite at different heights in the furnace and then burn out relatively quickly. In addition, the optical signals were weak and the deduced particle sizes were too small ($\sim 60 \mu\text{m}$) to be reliably measured with the coded aperture optical technique. It was deduced that the small apparent char particle sizes resulted from extensive devolatilization (small biomass particles can lose upwards of 90% of their mass to volatilization when heated rapidly to high temperatures) (Bharadwaj et

al., 2004). To overcome these difficulties, it was decided to feed a larger size fraction of milled residue (106-180 μm) and to use a high-temperature furnace environment of 1700 K, to minimize variations in the ignition height of different residue particles from a given sample and to provide a direct comparison with an extensive database of coal char reactivity information available at this temperature. Photographs of the combustion of these particles are shown in Fig. 15. While some optical particle measurements were possible, the variation in the ignition height of the particles, their rapid burnout, variable particle feed rates (because of difficulty feeding), and particle dispersion within the furnace (because of their high volatiles loss and the jetting action of volatiles) made the measurements inefficient, with consumption of much of the limited samples yielding only a few good optical measurements. The optical measurements did show a mean char particle size of $\sim 90 \mu\text{m}$, validating the choice of particle sizes in the feed.

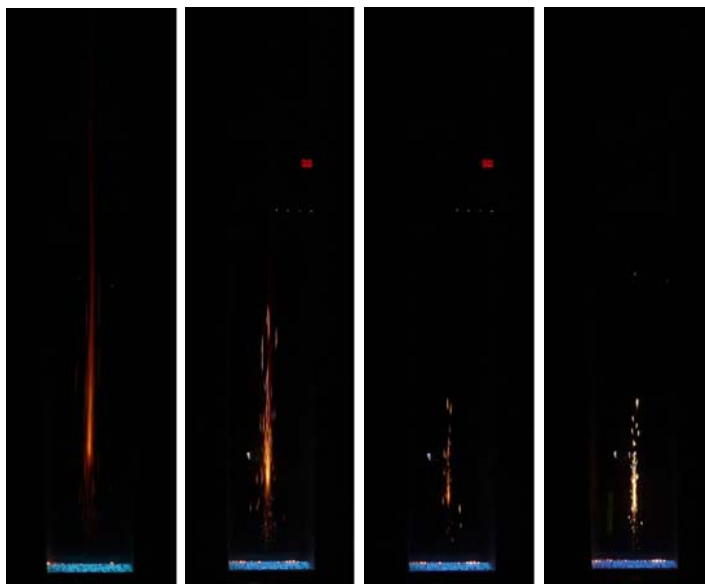


Figure 14. Photographs of 75-106 μm corn stover SAA lignin residue burning in a 1200 K furnace with 12%, 24%, 36%, and 60% O_2 , respectively.

Improved Combustion Characterization

To improve upon both the quality and quantity of optical data collected, we decided to devolatilize the residue particles in an electrically heated, downflow, enclosed reactor known as the Pressure-Capable Entrained Flow Reactor (PCEFR), shown in Fig. 16. These devolatilized particles were then fed into the optical entrained flow reactor for characterization of their combustion reactivity. By devolatilizing the particles before feeding into the combustion reactor, the particles tend to stay at the reactor centerline, leading to more efficient capture of optical data. Also, as demonstrated recently in a separately funded project evaluating coal particle combustion, pre-generation of char particles removes the effect of variations in the devolatilization process in the optical entrained flow reactor when raw particles are fed into environments with different oxygen concentrations. For the lignin residues (and for their associated raw biomass feedstock), a particle size range of 75-180 μm was fed into the PCEFR

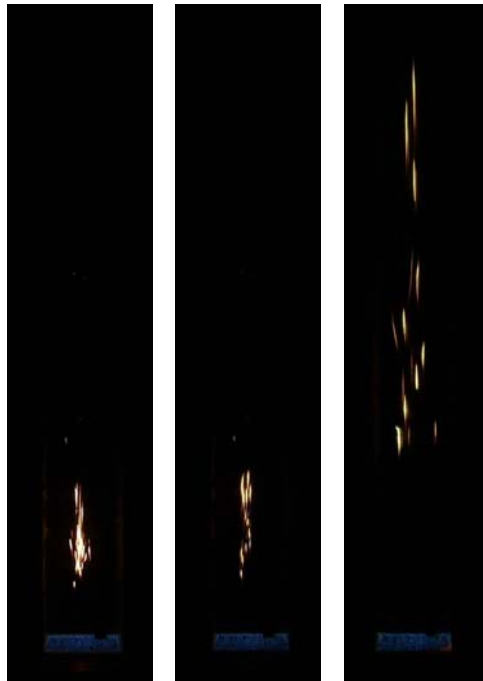


Figure 15. Photographs of 106-180 μm particles of different lignin residues burning in 36% O_2 in a 1700 K furnace. The leftmost two photos show two different corn stover SAA pretreatment residues and the rightmost photo shows a eucalyptus SAA process residue.

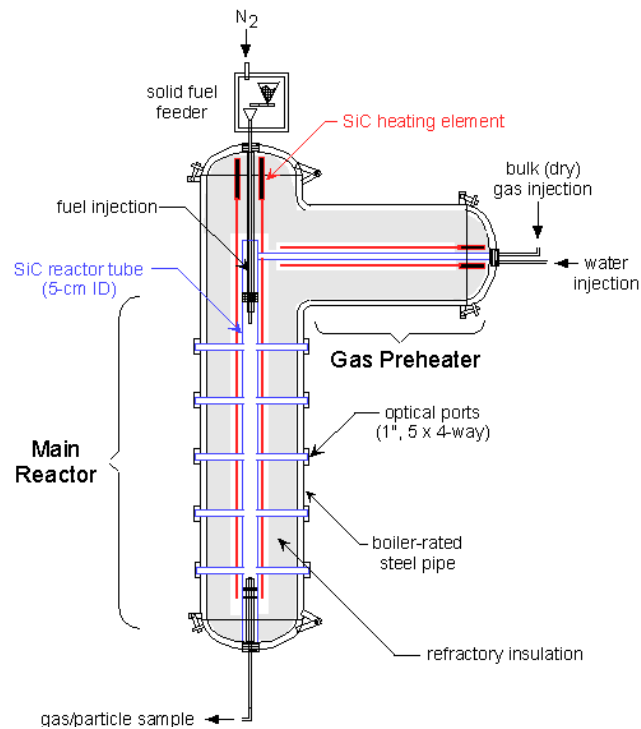


Figure 16. Schematic of Sandia's Pressure-Capable Entrained Flow Reactor (PCEFR).

when flowing N_2 at $1200\text{ }^\circ\text{C}$, and the collected char particles were received to $75\text{-}106\text{ }\mu\text{m}$ for feeding into the optical EFR.

Analysis of the volatile yield from the lignin residue particles is awaiting completion of commercial lab analysis of the ash content of the char samples and will be reported in a subsequent journal article on this work. Similarly, we are awaiting the results of full proximate/ultimate analysis of the residues themselves. Photographs of the combustion of the eucalyptus char and those of its Arkenol residues in the optical EFR at 1700 K are shown in Fig. 17, together with photographs of corn stover residues directly fed into the furnace. Unfortunately, there was insufficient corn stover residue sample to generate enough char material for optical characterization of the combustion of the char feed. The differences in apparent burnout height of the different char materials probably reflect differences in densities of the chars, because the char samples were sieved to be in the same initial size range. A denser particle of the same size as another will inherently take longer to burn out, simply because there is more carbonaceous mass to consume. On this basis, it appears that the raw eucalyptus char particles are substantially lighter than those produced from the Arkenol-pretreated eucalyptus. The SAA pretreated corn stover particles burn out very quickly, while those from the SSF process take substantially longer to burn, possibly reflecting the $\sim 16\%$ ash in these particles (typ. analysis provided by NREL). The raw eucalyptus char and, especially, the SSF residue, show substantial yellow emission in a wide band extending outside of the burning particles. This

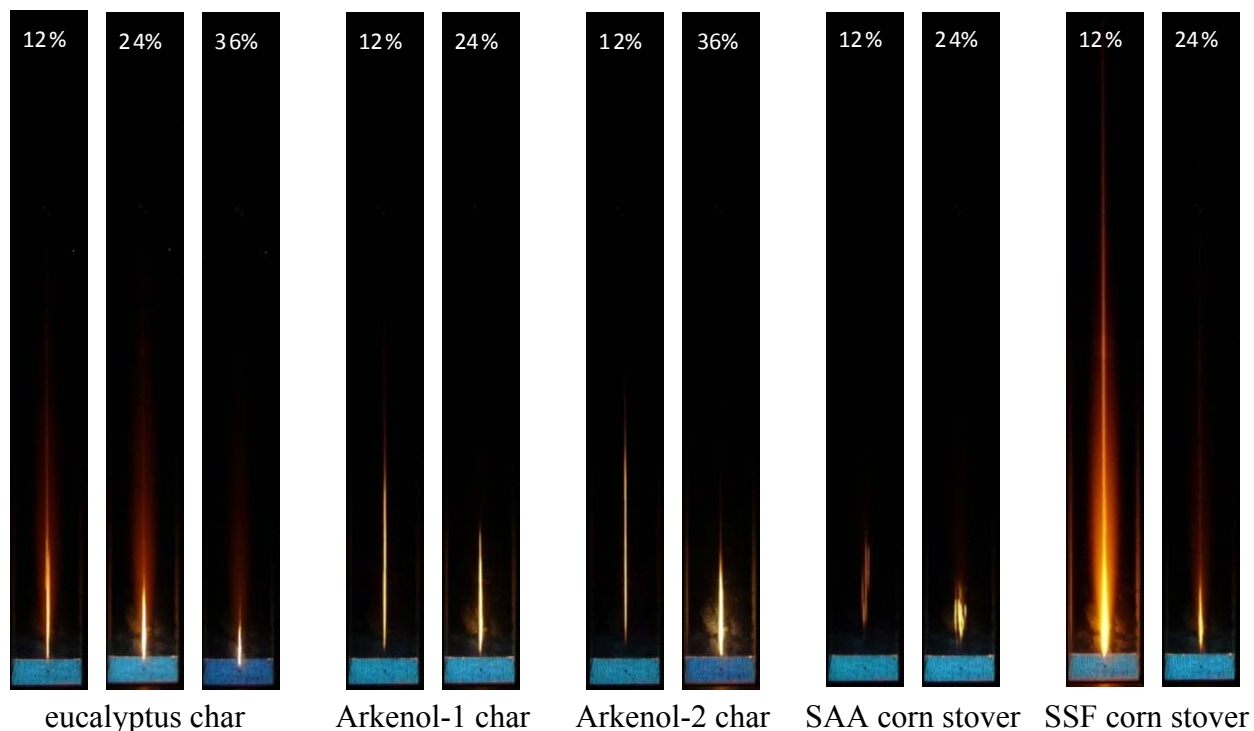


Figure 17. Photographs of combustion of chars generated from raw and Arkenol-pretreated eucalyptus and of direct combustion of residues from pretreated corn stover in the optical EFR at 1700 K . “%” labels refer to oxygen content of flow. “Arkenol-1” refers to single-step hydrolysis and “Arkenol-2” refers to dual-step hydrolysis.

observation in the optical EFR is typically associated with Na release from the particles. The results of ash analysis of the feedstocks and the different residues should confirm the presence of significant sodium in the eucalyptus and in the SSF corn stover residue. The strong sulfuric acid Arkenol pretreatment undoubtedly removes alkali metals from the eucalyptus and carries them in the acid-sugar solution. In the SAA pretreatment, the alkali metals probably remain with the solids and thus are segregated from the lignin residue that is produced from the ammonia wash.

In a given combustion environment, similar-size particles will burn at different temperatures according to the rate at which they are reacting. The oxidation of carbon and hydrogen components of the char particle releases energy, such that the more quickly a particle burns, the greater its combustion temperature (Glassman and Yetter, 2009). This fact can be used to evaluate the relative reactivity of different fuels, based on their combustion temperatures in a given environment, or, with a detailed energy balance, can be used to derive overall char combustion kinetic rate parameters (Murphy and Shaddix, 2006). Mean char particle temperature measurements for the various residues are shown in Figs. 18 and 19, as a function of height above the burner in the optical EFR. Fig. 18 shows that the SSF residue has substantially lower reactivity than the SAA residue., which might be attributed, at least in part, to the significant ash content of the SSF residue. Fig. 19 shows that the raw eucalyptus has slightly higher reactivity than the Arkenol residues, as one might expect. Somewhat surprisingly, the one-pass and two-pass Arkenol residues show nearly identical particle combustion temperatures, suggesting little chemical difference in the chars formed from these residues with different degrees of hydrolytic removal of carbohydrates.

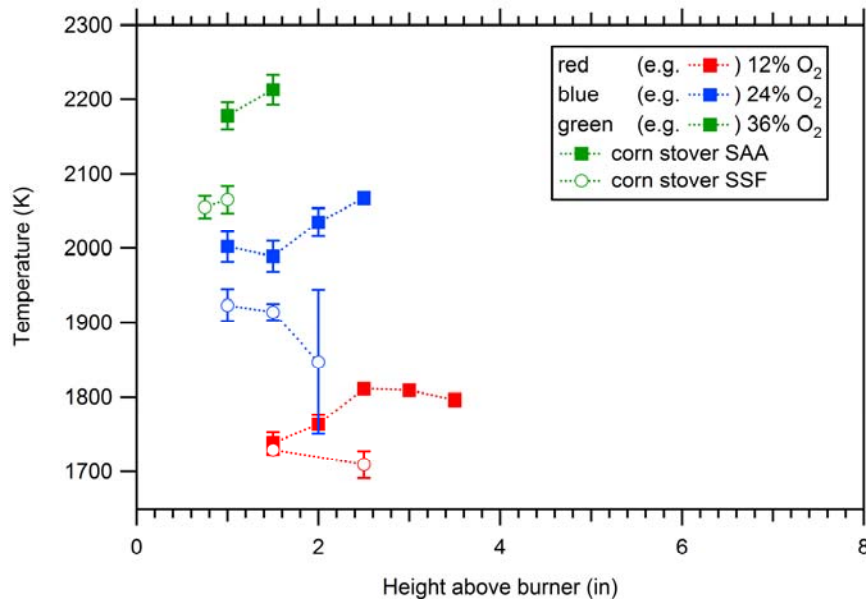


Figure 18. Mean corn stover residue char combustion particle temperatures measured as a function of height in Sandia’s optical EFR when operating at 1700 K.

From the profiles shown in Figs. 18 and 19, the peak mean particle temperatures can be used as a measure of the characteristic particle reactivity, specifically relative to oxygen as an oxidizer, but

also more generally towards any gasifying reactant, whether it is oxygen, carbon dioxide, or steam. In this way, the reactivity of these residues in comparison to typical coals used in combustors and gasifiers can be evaluated. Fig. 20 shows a comparison of the peak mean particle temperatures from the biomass residue chars in comparison to those previously measured for the full rank spectrum of pulverized coal, ranging from the most reactive coals, lignite, to the least reactive, anthracite (Shaddix et al., 2009). Because of the similarity in peak mean temperatures for the one-pass and two-pass Arkenol residues, a single profile for Arkenol residues is shown in Fig. 20.

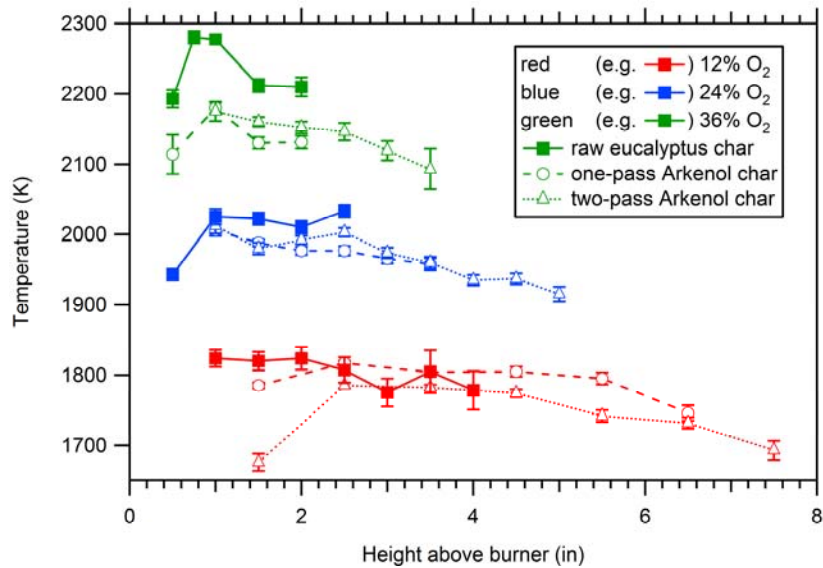


Figure 19. Mean eucalyptus residue char combustion particle temperatures measured as a function of height in Sandia's optical EFR when operating at 1700 K.

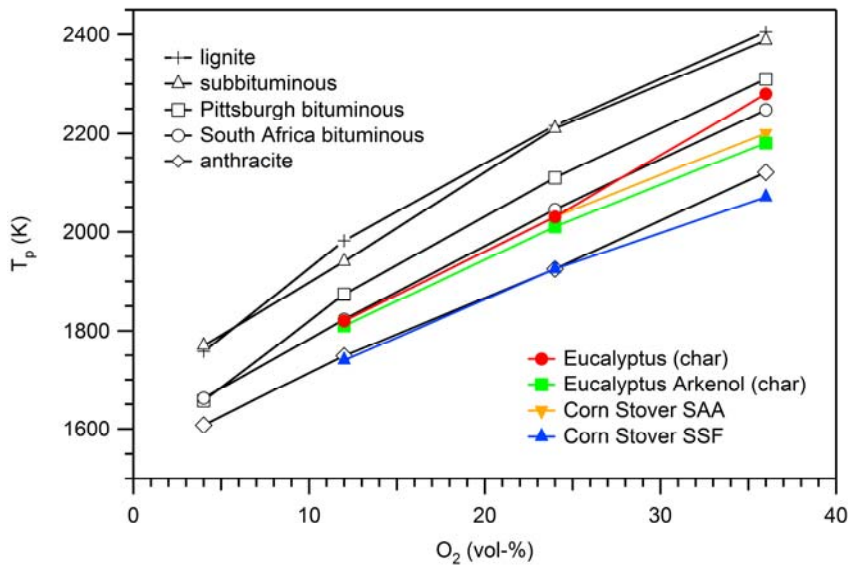


Figure 20. Mean corn stover residue char combustion particle temperatures measured as a function of height in Sandia's optical EFR when operating at 1700 K.

Not unexpectedly, the char formed from the raw eucalyptus has the highest reactivity of all of the biomass samples investigated. The SAA treated corn stover and the Arkenol process eucalyptus char particles have very similar reactivities, while the SSF process corn stover residue has a substantially lower reactivity. The overall rank position of the biomass chars is surprising. Normally one would expect raw biomass to have at least as great a reactivity as lignite. However, the eucalyptus chars were prepared *ex situ*, in the PCEFR, with a residence time of over 1 second, which may decrease the reactivity compared to an *in situ* formed char. Also, in support of the findings here, Wornat et al. (1996) measured the combustion reactivity of two different biomass chars (from Southern pine and switchgrass) that were produced from flash pyrolysis of biomass at 625 °C and found them to be equivalent to *in situ* formed high-volatile bituminous coal chars (such as the Pittsburgh and South Africa coals shown in Fig. 20). Of course, one caveat to this comparison of apparent reactivities of the biomass chars and coal chars is that the coal chars tend to be largely spherical, whereas the biomass-derived chars (for all but the SAA-treated corn stover) tend to have disparate aspect ratios along the plant grain, which facilitates heat transfer from the particle to the surrounding gas and thereby lowers their apparent reactivity relative to coal chars. This consideration requires further study to help quantify this effect for the different biomass samples. Furthermore, a calibration check performed after completion of the biomass sample measurements shows that the two-color pyrometer calibration constant needs to be adjusted upward for the biomass data – this correction is in the process of being fully quantified.

System Analysis

Work on this portion of the project began by conducting an exergy analysis of a canonical thermochemical process for lignocellulosic ethanol production that has been evaluated by NREL using ASPEN Plus software. After this, an exergy and enthalpy analysis was conducted on a canonical biochemical process for cellulosic ethanol production. In addition, a detailed analysis was conducted of the biochemical fermentation process with baker's yeast, a commonly used fermentation organism.

Thermochemical Ethanol System

NREL researchers analyzed the hypothetical performance of a lignocellulosic ethanol plant based on indirect gasification of wood chips with subsequent tar reforming, syngas cleanup, syngas compression, and finally mixed alcohol production over a catalyst (Phillips et al., 2007; Phillips 2007). A schematic of this system is shown in Fig. 21. In the LDRD project, an exergy balance for the NREL process model for thermochemical biomass-to-ethanol conversion was constructed, in collaboration with NREL researchers, from the input and output process variables in the ASPEN Plus model of the system that was developed at NREL. NREL has conducted “state-of-the-art” analyses of the system based on evaluations of current technology in 2007 and 2008, as well as projected improvements that are targeted to be available by 2012. The projected, 2012 performance is considered the default design case. A comparison of the overall energy budget and overall exergy budget for the 2012 design case is shown in Fig. 22. The exergy balance is based on an evaluation of the ability of the system to “do work” and thereby is a more meaningful measure of system efficiency than can be gleaned from an energy balance, which

the system, the exergy analysis shows that the gasification process and the tar reforming step are the primary sources of inefficiency, totaling over 30% of the input exergy and over 50% of the exergy ‘loss’ in the system. In contrast, the heat transfer losses that dominate the energy losses in the system only amount to 6% of the exergy budget, because of the preponderance of low-grade heat that has limited ability to do work.

Further insights are gained by looking at the energy and exergy budgets of the individual process steps. The low-temperature, low-pressure (1270 K, 1.7 atm) indirect steam gasifier was found to have an exergetic efficiency of 71%, as shown in Fig. 23. In comparison, the NREL study determined that the gasifier first-law efficiency was 76%. The exergy analysis showed that approximately one-half of the exergy loss was associated with the gasifier itself and half with the char combustor. A significant amount of the input exergy (9%) is contained in the flue gas, so there exists the opportunity to improve the efficiency of this process with additional heat recovery from the flue. The extensive production of hydrocarbons in this low-temperature gasifier represents a significant fraction of the system exergy (~ 1/3 of the input exergy).

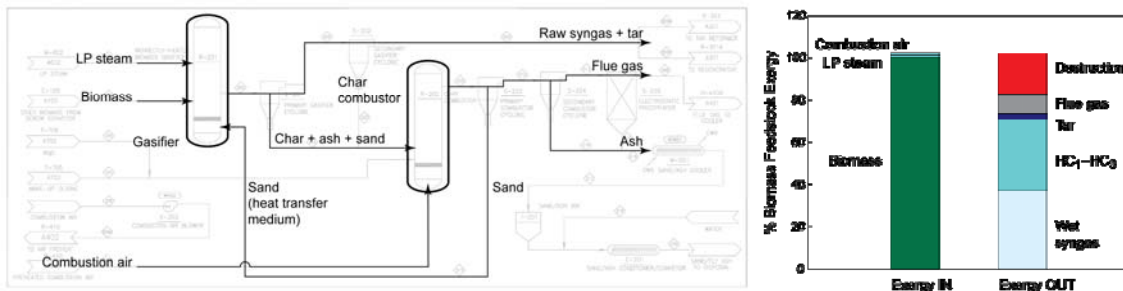


Figure 23. (Left) The dual-bed, indirect steam gasifier model overlaid on the NREL process flow diagram. (Right) Gasifier system exergy inputs and outputs.

An analysis was also conducted of the influence of the indirect gasifier operating temperature on exergy loss. For this analysis the presumed amount of char combustion excess air was varied (from the 20% excess assumed in the NREL analysis) and the fuel feed and steam inputs were assumed constant. NREL correlations for syngas and char composition versus temperature were used, and the two reactors were assumed adiabatic. The results of this analysis are shown on the right side of Fig. 24. Reducing the combustion air supply from 20% to 10% in excess of the stoichiometric amount for complete char combustion raises the gasification temperature from 1605 °F to 1620 °F (874 °C to 882 °C), and adiabatic char combustion temperature from 2190 °F to 2220 °F (1200 °C to 1215 °C). Correspondingly, the exergy destruction decreases from 9% to 8.5% of feedstock exergy. Lowering the steam-to-feedstock ratio (set at 0.4 kg/kg in NREL studies) serves the same purpose of raising operating temperature and reducing exergy destruction. In fact, for high temperature entrained flow gasifiers, for which the syngas approaches chemical equilibrium (Kovacik et al., 1990), one can show that the gasification process has to be carried out at the highest possible energy state (highest temperature, pressure) to minimize exergy destruction. The analytical proof was solved for internal combustion engines (Teh et al., 2008), but the results may also be extended to gasification. However, in the latter case, one needs to weigh the exergy destruction minimization/efficiency maximization objective of the gasification process without losing sight of its primary function, which is to supply syngas

of certain desired characteristics (e.g., H_2 -to-CO ratio) for the synthesis step downstream. Also, high temperature gasification systems for producing syngas generally require the use of oxygen as a reactant, and the impact of oxygen generation on the overall process exergy budget would need to be evaluated.

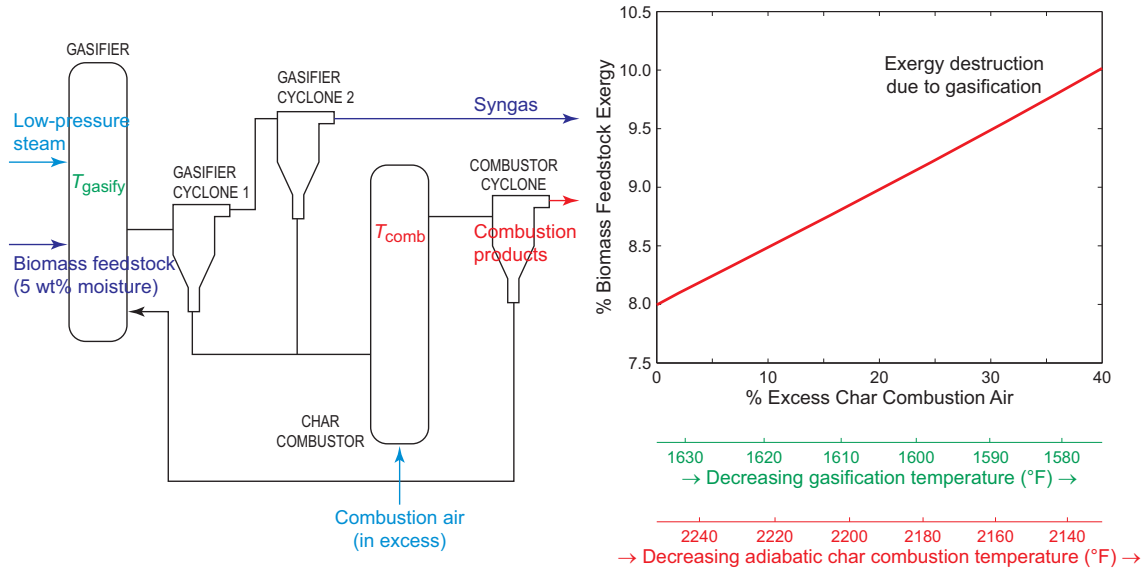


Figure 24. Schematic of the modeled gasifier block system (left) and the calculated exergy loss of the system as a function of the excess air supplied to the char combustor (right).

The alcohol synthesis reactor was modeled as a high- P , isothermal (570 K, 67 atm) process akin to the Fischer-Tropsch process, but using a sulfided molybdenum catalyst (MoS_2). Using the catalyst performance targets specified by NREL, the synthesis process was found to be nearly reversible: only 2% exergy input is destroyed and the process has an overall exergetic efficiency of 95% (see Fig. 25). The NREL performance targets specify 60% CO conversion (*cf.* state-of-technology: 10–40%) and 90% alcohol selectivity (*cf.* state-of-technology: 70–80%). Given the aggressive performance targets and the proximity of the resultant process to an ideal, reversible

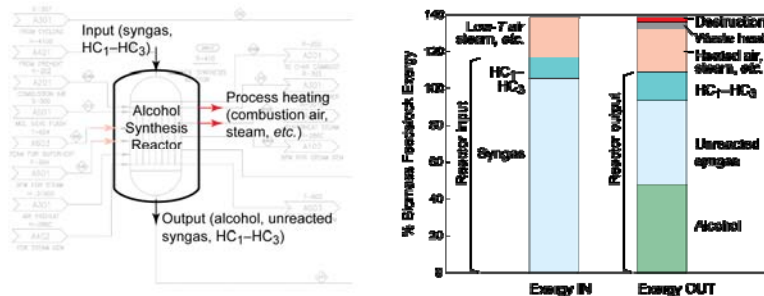


Figure 25. (Left) The alcohol synthesis reactor overlaid on the NREL process flow diagram. (Right) Synthesis reactor exergy inputs and outputs.

process, it appears that the NREL performance targets are probably too optimistic to be achievable.

Figure 22 shows that feedstock drying represents a 6% exergy loss from the system. To evaluate the potential for reducing this inefficiency, calculations were performed for the wood chip dryer as a function of the moisture content of the feed and the inlet air temperature to the dryer, while holding the dried wood moisture content (5%) and dried wood and air exit temperatures (220 °F and 230 °F) constant (see Fig. 26). The system was assumed to be adiabatic (i.e. no heat losses through the walls). With these assumptions, the exergy loss is seen to be a strong function of the moisture content of the raw feedstock. Lowering raw feedstock moisture level from 50 wt%, per NREL studies, to 40 wt%, for instance, would reduce exergy destruction by a third. At a 20 wt% moisture content—near the level for air-dried lumber—the exergy destroyed drops to about 1% of biomass feedstock exergy. The drying process efficiency also increases, albeit to a much smaller extent, with decreasing inlet air temperature, i.e., accomplished using sensible energy/thermal resource of lower quality—but at a higher quantity. At 50 wt% moisture level, decreasing the inlet air temperature from 1200 °F to 900 °F (650 °C to 480 °C), while increasing the flow rate accordingly, reduces the exergy destroyed by 10%. The trend diminishes at lower moisture levels.

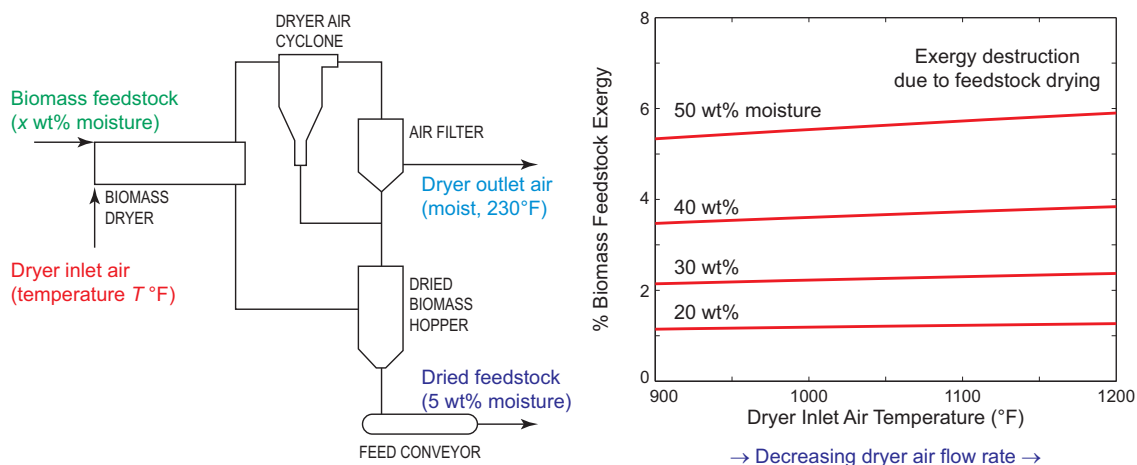


Figure 26. Schematic of the modeled wood dryer block system (left) and the calculated exergy loss of the system as a function of the inlet air temperature (right).

In addition to this detailed examination of the 2012 thermochemical process design case, overall evaluations were also performed of the 2007 and 2008 “State of Technology” evaluations that were performed by NREL using ASPEN Plus. This analysis allowed a quantitative assessment of the impact of the thermochemical process performance improvements projected by NREL on the production of ethanol and higher alcohols and is summarized in Fig. 27. By reducing exergy losses, the exergetic efficiency of producing ethanol and higher alcohol is seen to progress from 24% in 2007 to 31% in 2008 and 42% in 2012. From 2007 to 2008 there is a significant drop in the exergy losses associated with CO₂ separation and process heating. From 2008 to 2012,

significant reductions in exergy loss associated with tar reforming and syngas compression are forecast, based on improvements in catalyst activity and selectivity.

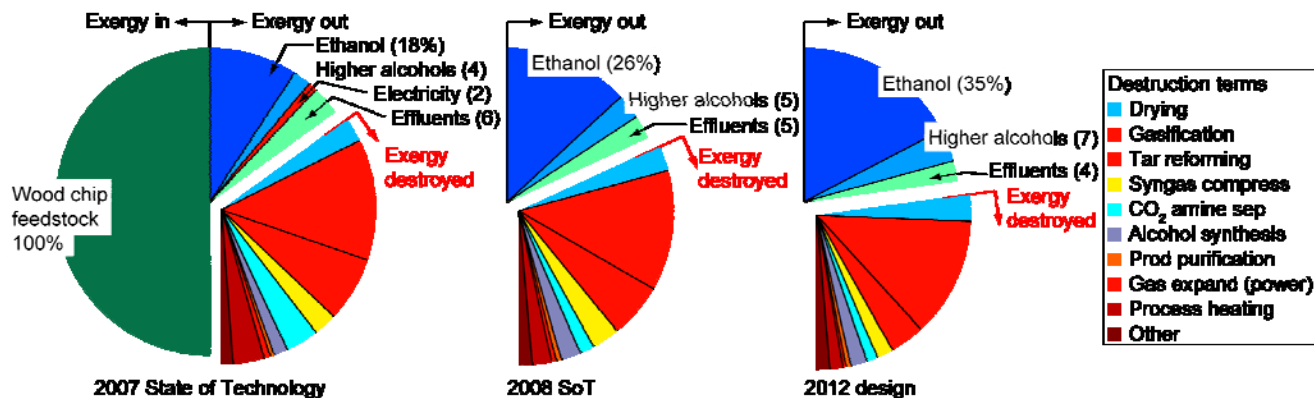


Figure 27. Exergy budget for the thermochemical ethanol design case using 2007 and 2008 “state of technology” performance assumptions and the target 2012 design case.

Biochemical Ethanol System

We analyzed the efficiency of biomass-to-ethanol fuel production based on prototypical biochemical conversion technologies (using either hot water or dilute acid pretreatment followed by enzymatic hydrolysis – see Fig. 28). We considered three representative scenarios developed for a 2009 National Research Council study on alternative liquid transportation fuels (National Research Council, 2009). The critical assumptions used for the three different scenarios are shown in Table 1. The “low-performance” scenario represents current technology; “medium-performance” represents where the technology is likely to be after reasonable, evolutionary advancements (by 2020); “high-performance” represents the most optimistic technology advancements (as a limiting case). Thus, the low-performance and high-performance scenarios provide realistic bounds on the expected behavior of a dedicated biochemical ethanol plant.

Table 1: Assumptions for NRC Low-, Medium-, and High-Performance Processes

Variable	Low	Medium	High
Solids loading	18%	21%	25%
Pretreatment yield	80%	85%	95%
Saccharification extent	90%	95%	95%
Fermentation yield, glucose	85%	90%	90%
Fermentation yield, xylose	75%	81%	81%

The results of our energy and exergy analysis of this process for the low-performance scenario are shown in Figure 29. The process efficiency (considering ethanol and electricity as the desirable outputs) is 38% based on an energy balance and 33% based on the exergy balance. Heat

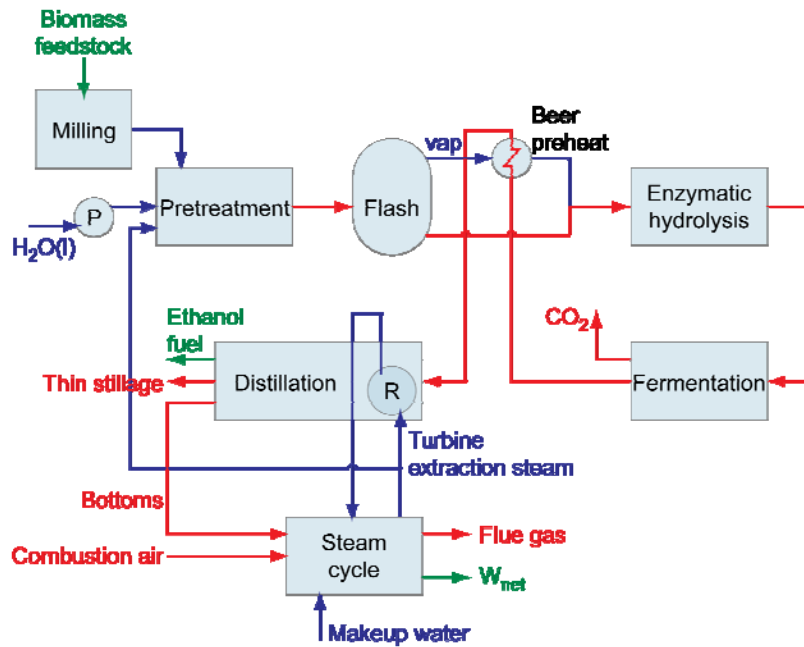


Figure 28. Schematic of a prototypical lignocellulosic biochemical ethanol plant, utilizing separate enzymatic hydrolysis and fermentation steps.

loss is the principal source of energy loss, whereas the steam cycle is the primary source of exergy loss (i.e. is the primary source of inefficiency in the system). At first glance, it would appear that exergy destruction is low for all the biochemical sub-processes (pretreatment, enzymatic hydrolysis, and fermentation), as well as ethanol distillation. However, it should be noted that the exergetically inefficient steam cycle serves to meet the steam and power demands of the pretreatment, distillation, and feedstock size reduction steps.

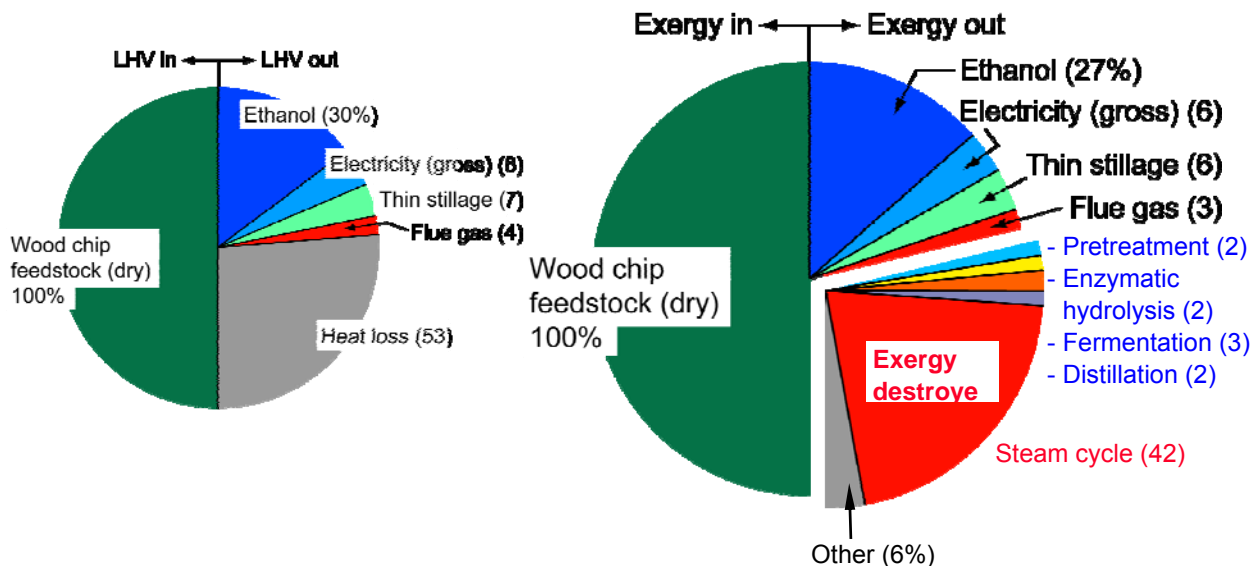


Figure 29. Energy inputs and outputs (left pie chart) and exergy inputs and outputs (right pie chart) for the "low-performance" biochemical process design case.

Figure 30 shows the exergy budget implications of the expected evolution of the current biochemical process technology to future idealized process states. The overall exergetic efficiency improves from 33% (using current “low” technology) to 38%, with a possible further improvement to 42% (under the most optimistic “high” technology assumption). The primary source of this efficiency improvement lies in reduced steam generation requirements.

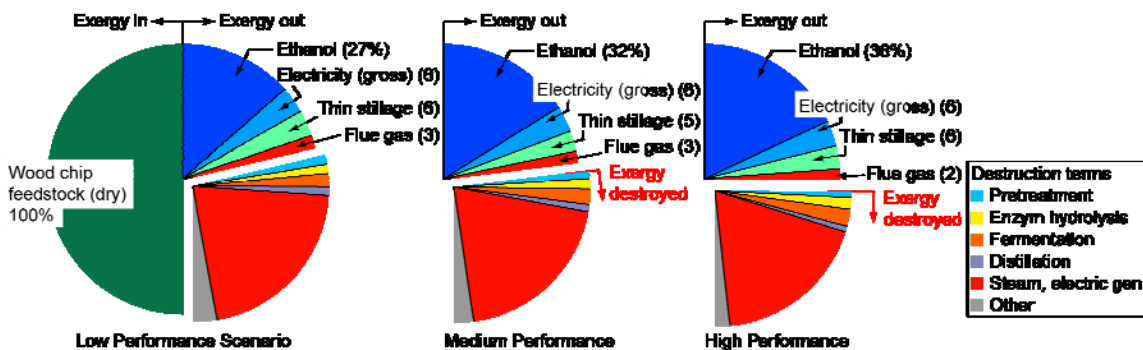


Figure 30. Exergy budget for the prototypical biochemical conversion process based on NRC technology performance scenarios.

The large exergy loss associated with the steam cycle has implication for the potential integration of the bio- and thermo-chemical approaches to produce lignocellulosic ethanol, since the process steam and electricity needs reduce the availability of lignin-rich residue (from the biochemical conversion process) as feedstock for subsequent thermochemical conversion to fuel. The steam requirements for ethanol distillation may decrease significantly in the future, with the commercial adoption of membrane vapor permeation technology. The projected energy consumption of this distillation technology is approximately one-third the energy consumption of conventional, low-capital cost distillation and dehydration technology, as shown in Fig. 31.

The heating value of the available lignin residue provides a quantitative measure to investigate the feasibility of an integrated bio-/thermo-chemical biofuel production concept. Figure 32 illustrates the trade-off between available residue heating value and gross electricity production, after steam requirements for pretreatment and distillation processes have been satisfied. Estimates of electricity use during biochemical fuel production vary widely, depending on the assumed system configuration and scale, feedstock, etc. For instance, two NREL process designs specified electricity consumption per gallon ethanol production to be, respectively, 1.4 kWh and 5.3 kWh (equivalent to 0.5 MJ and 1.4 MJ per kg dry biomass feedstock). As shown in Figure 32, our analysis indicates that electricity use at the high end would leave little excess lignin-rich residue for thermochemical fuel production, assuming that electricity is co-generated (with steam) via combustion of the residue. Available, excess residue increases by 3% to 4% of original feedstock LHV if the process steam requirement for ethanol separation decreases based on more-advanced membrane vapor permeation technologies. On the other hand, advances in biochemical fuel production (based on NRC technology outlook) would mean better utilization of feedstock sugars, leaving smaller quantities of recalcitrant (unhydrolyzed) cellulose and hemicellulose in the residue for additional thermochemical production of biofuel. Assuming that the USDA or lower NREL estimate for electricity requirement is accurate, residue with around

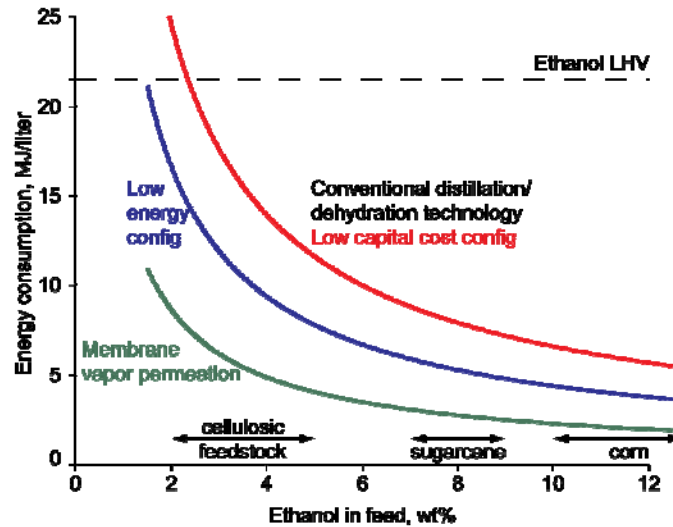


Figure 31. Energy consumption for ethanol distillation as a function of the ethanol in the feed to the distillation process and the technology employed (data from Madson and Lococo, 2000; Vane, 2008; Cote et al., 2008).

20–30% of the original biomass feedstock LHV content may be diverted from electricity generation and made available for thermochemical biofuel production. Furthermore, if improvements are made in the pretreatment process that reduce the pressure and quantity of steam required for pretreatment even larger amounts of the feedstock LHV will be available for thermochemical processing.

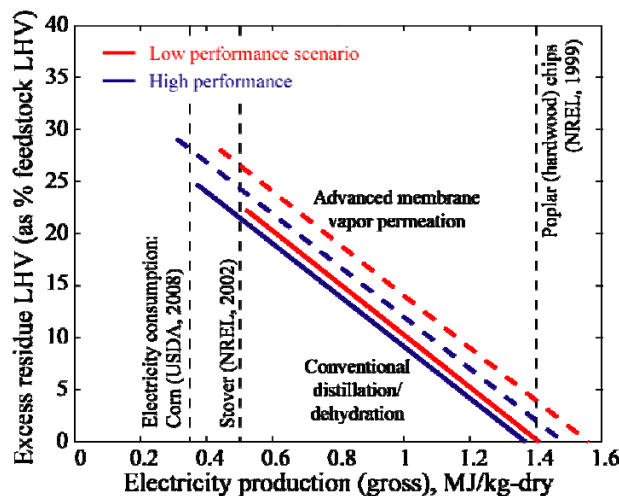


Figure 32. Trade-off between electricity and thermochemical biofuel production using lignin-rich residue from a prototypical biochemical conversion process.

Baker's Yeast Fermentation

We analyzed the thermodynamics of microbial growth with respect to fermentation of glucose to ethanol by baker's yeast (*S. cerevisiae*), a model fermentation organism with a well-understood metabolism. The model couples a detailed cellular metabolic flux analysis with bulk changes across a fermentation reactor, as shown schematically in Fig. 33. Results of this work have been published by Teh and Lutz (2010) and will therefore only be briefly summarized here. The exergy analysis showed that the anaerobic metabolism of yeast is very efficient, retaining more than 90% of the exergy of the growth medium. However, a portion of the metabolism is devoted to cellular production and to the generation of metabolic by-products other than ethanol, such that the glucose-to-ethanol efficiency is less than 75%. Fig. 34 shows these results as a function of ATP consumption, which reflects the extent of cell stress/activity.

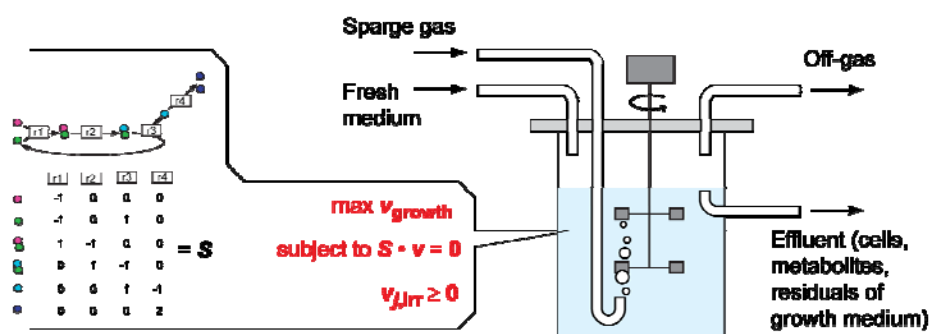


Figure 33. Schematic of modeled system of continuous culture of baker's yeast fermenting glucose under anaerobic, glucose-limited conditions.

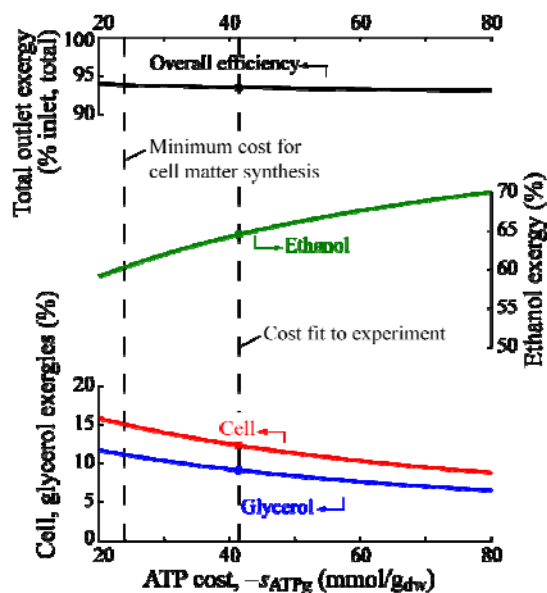


Figure 34. Exergetic efficiencies of fermentation process, as a function of the cellular ATP consumption.

Conclusions

In this LDRD project, research was performed on pretreatment strategies to remove lignin from lignocellulosic feedstocks, on the thermochemical conversion characteristics of such lignin-rich residues, and on using exergy analysis to identify inefficiencies in thermochemical and biochemical approaches to cellulosic ethanol production. The overall goal of this work was to lay the foundation for more efficient and more productive conversion of lignocellulosic feedstocks to ethanol via an integrated process wherein excess lignin-rich residues from the base biochemical process are processed thermochemically to yield additional liquid fuel or high-efficiency electricity.

Two existing pretreatment approaches, soaking in aqueous ammonia (SAA) and the Arkenol process (utilizing strong sulfuric acid), were implemented and used to generate sufficient residue material from corn stover and eucalyptus feedstocks for subsequent thermochemical research. Ionic liquid (IL) processing of biomass was investigated by Sandia researchers at the Joint Bioenergy Institute (JBEI), but was not successful in isolating sufficient lignin residue for thermochemical characterization. Additional residue material for thermochemical research was supplied from the dilute-acid simultaneous saccharification/fermentation (SSF) pilot-scale process at the National Renewable Energy Laboratory (NREL). The high-temperature volatiles yields of the different residues were measured, as well as the char combustion reactivities. The residue chars showed slightly lower reactivity than raw biomass char, except for the SSF residue, which had substantially lower reactivity.

Exergy analysis was applied to the NREL standard process design model for cellulosic ethanol production from a dedicated thermochemical process (utilizing an indirect gasifier) and from a prototypical dedicated biochemical process, with process data supplied by a recent report from the National Research Council (NRC). The thermochemical system analysis revealed that most of the system inefficiency is associated with the gasification process and subsequent tar reforming step. For the biochemical process, the steam generation from residue combustion, providing the requisite heating for the conventional pretreatment and alcohol distillation processes, was shown to dominate the exergy loss. An overall energy balance with different potential distillation energy requirements shows that as much as 30% of the biomass energy content may be available in the future as a feedstock for thermochemical production of liquid fuels.

List of References

- P. Alvira, E. Tomás-Pejó, M. Ballesteros, M. J. Negrero, "Pretreatment technologies for an efficient bioethanol production process based on enzymatic hydrolysis: a review," *Biores. Technol.* 101:4851-4861 (2010).
- A. Bharadwaj, L.L. Baxter, A.L. Robinson, "Effects of intraparticle heat and mass transfer on biomass devolatilization: experimental results and model predictions," *Energy Fuels* 18:1021-1031 (2004).
- S.L. Blunk, B.M. Jenkins, "Combustion properties of lignin residue from lignocellulosic fermentation," Report prepared for National Renewable Energy Laboratory, NREL Subcontract ACG-8-18021-01, April 2000.
- P. Cote, G. Noel, S. Kroll, M. Schwartz, M. Kazmir, "From design to operation of a 2 Mgal/y membrane-based ethanol dewatering system," Fuel Ethanol Workshop, 2008.
- J.C. Cuzens, J.R. Miller, "Acid hydrolysis of bagasse for ethanol production," *Renewable Energy* 10:285-290 (1997).
- D.C. Dibble, C. Li, L. Sun, A. George, A. Cheng, Ö.P. Çetinkol, P. Benke, S. Singh, B.A. Simmons, "Ionic liquid pretreatment with gel-free precipitation and IL recycling utilizing a phase-switchable solvent system," submitted to *Green Chemistry* (2010).
- I. Dincer, "The role of exergy in energy policy making," *Energy Policy* 30:137-149 (2002).
- G. Eriksson, G. Kjellström, B. Lundqvist, S. Paulrud, "Combustion of wood hydrolysis residue in a 150 kW powder burner," *Fuel* 83:1635-1641 (2004).
- W.A. Farone, J.E. Cuzens, U.S. patent no. 5,620,877 (1997).
- W.A. Farone, J.E. Cuzens, U.S. patent no. 5,726,046 (1998).
- I. Glassman, R.A. Yetter, *Combustion*, 4th Ed., Academic Press: Amsterdam, 2008, pp. 531-542.
- J.N. Himmelsbach, A. Isci, D.R. Raman, R.P. Anex, "Design and testing of a pilot-scale aqueous ammonia soaking biomass pretreatment system," *Appl. Engin. Agric.* 25:953-959 (2009).
- H. Kim, J. Ralph, "Solution-state 2D NMR of ball-milled plant cell walls in DMSO-*d*₆/pyridine-*d*₅," *Org. Biomol. Chem.* 8:576-591 (2010).
- H. Kim, J. Ralph, T. Akiyama, "Solution-state 2D NMR of ball-milled plant cell walls in DMSO-*d*₆," *Bioenergy Res.* 1:56-66 (2009).
- T.H. Kim, J.S. Kim, C. Sunwoo, Y.Y. Lee, "Pretreatment of corn stover by aqueous ammonia," *Biores. Technol.* 90:39-47 (2003).

- T.H. Kim, Y.Y. Lee, "Pretreatment of corn stover by soaking in aqueous ammonia," *Biores. Technol.* 121-124:1119-1132 (2005).
- T.H. Kim, Y.Y. Lee, "Pretreatment of corn stover by soaking in aqueous ammonia at moderate temperatures," *Biores. Technol.* 136-140:81-92 (2007).
- T.H. Kim, F. Taylor, K. Hicks, "Bioethanol production from barley hull using SAA (soaking in aqueous ammonia) pretreatment," *Biores. Technol.* 99:5694-5702 (2008).
- G. Kovacic, M. Oguztoreli, A. Chambers, B. Ozum, "Equilibrium Calculations in Coal Gasification," *Int. J. Hydrogen Energy* 15:125-131 (1990).
- P. Kumar, D.M. Barrett, M.J. Delwiche, P. Stroeve, "Methods for pretreatment of lignocellulosic biomass for efficient hydrolysis and biofuel production," *Ind. Eng. Chem. Res.* 48:3713-3729 (2009).
- W.-Z. Li, Y.-J. Yan, T.-C. Li, Z.-W. Ren, M. Huang, J. Wang, M.-Q. Chen, Z.-C. Tan, "Preparation of hydrogen via catalytic gasification of residues from biomass hydrolysis with a novel high strength catalyst," *Energy Fuels* 22:1233-1238 (2008).
- X. Li, T.H. Kim, N.P. Nghiem, "Bioethanol production from corn stover using aqueous ammonia pretreatment and two-phase simultaneous saccharification and fermentation (TPSSF)," *Biores. Technol.* 101:5910-5916 (2010).
- P.W. Madson, D.B. Lococo, "Recovery of volatile products from dilute high-fouling process streams," *Appl. Biochem. Biotech.* 84-86:1049-1061 (2000).
- J.J. Murphy, C.R. Shaddix, *Combust. Flame* 144:710-729 (2006).
- National Research Council, Liquid Transportation Fuels from Coal and Biomass: Technological Status, Costs, and Environmental Impacts, National Academies Press, ISBN: 978-0-309-13712-6, 2009.
- M. Öhman, C. Boman, H. Hedman, R. Eklund, "Residential combustion performance of pelletized hydrolysis residue from lignocellulosic ethanol production," *Energy Fuels* 20:1298-1304 (2006).
- H. Ohno, Y. Fukaya, "Task specific ionic liquids for cellulose technology," *Chem. Lett.* 38:2-7 (2009).
- R.D. Perlack, L.L. Wright, A.F. Turhollow, R.L. Graham, B.J. Stokes, D.C. Erbach, "Biomass as Feedstock for a Bioenergy and Bioproducts Industry: The Technical Feasibility of a Billion-Ton Annual Supply," ORNL/TM-2005/66, April 2005.
- S.D. Phillips, "Technoeconomic analysis of a lignocellulosic biomass indirect gasification process to make ethanol via mixed alcohol synthesis," *Ind. Eng. Chem. Res.* 46:8887-8897 (2007).

- S. Phillips, A. Aden, J. Jechura, D. Dayton, T. Eggeman, "Thermochemical ethanol via indirect gasification and mixed alcohol synthesis of lignocellulosic biomass," Technical Report, NREL/TP-510-41168, April 2007.
- M.A. Rosen, C.A. Bulucea, "Using exergy to understand and improve the efficiency of electrical power technologies," *Entropy* 11:820-835 (2009).
- M.A. Rosen, I. Dincer, M. Kanoglu, "Role of exergy in increasing efficiency and sustainability and reducing environmental impact," *Energy Policy* 36:128-137 (2008).
- C.R. Shaddix, E.S. Hecht, S. Jimenez, S.M. Lee, "Evaluation of rank effects and gas temperature on coal char burning rates during oxy-fuel combustion," Proceedings of the 34th International Technical Conference on Coal Utilization and Fuel Systems, Clearwater FL, May 31 – June 4, 2009.
- C. Sievers, M.B. Valenzuela-Olarte, T. Marziale, I. Musin, P.K. Agrawal, C.W. Jones, "Ionic-liquid-phase hydrolysis of pine wood," *Ind. Eng. Chem. Res.* 48:1277-1286 (2009).
- R.P. Swatloski, S.K. Spear, J.D. Holbrey, R.D. Rogers, "Dissolution of cellulose with ionic liquids," *J. Am. Chem. Soc.* 124:4974-4975 (2002).
- K.-Y. Teh, A.E. Lutz, "Thermodynamic analysis of fermentation and anaerobic growth of baker's yeast for ethanol production," *J. Biotech.* 147:80-87 (2010).
- K.-Y. Teh, S.L. Miller, C.F. Edwards, "Thermodynamic requirements for maximum internal combustion engine cycle efficiency. Part 1: optimal combustion strategy," *Int. J. Engine Res.* 9:449-465 (2008).
- L.M. Vane, "Separation technologies for the recovery and dehydration of alcohols from fermentation broths," *Biofuels Bioprod. Bioref.* 2:553-588 (2008).
- M.J. Wornat, R.H. Hurt, K.A. Davis, N.Y.C. Yang, "Single-particle combustion of two biomass chars," *Proc. Combust. Instit.* 26:3075-3083 (1996).
- T. Yamada, M.A. Fatigati, M. Zhang, "Performance of immobilized *Zymomonas mobilis* 31821 (pZB5) on actual hydrolysates produced by Arkenol technology," *Appl. Biochem. Biotech.* 98-100:899-907 (2002).
- H.H. Yoon, Z.W. Wu, Y.Y. Lee, "Ammonia-recycled percolation process for pretreatment of biomass feedstock," *Appl. Biochem. Biotech.* 51/52:5-19 (1995).

Appendix A

LDRD Project Presentations and Publications

“Thermodynamic analysis of fermentation and an aerobic growth of baker’s yeast,” K.-Y. Teh, *ASME International Mechanical Engineering Congress and Exposition (IMECE)*, Lake Buena Vista, FL, Nov. 2009.

“Fractionation and recovery of lignin, carbohydrates, and aliphatic components of biomass in an ionic liquid pretreatment process” Dean C. Dibble, Anthe George, Aurelia Cheng, Chenlin Li, Ozgul Persil, Seema Singh, Blake Simmons, ACS 2010 Spring Meeting, March 21-25, San Francisco CA.

“Comparative exergy analysis of NREL thermo-chemical biomass-to-ethanol process designs,” K.-Y. Teh, A.E. Lutz, C.R. Shaddix, A. Dutta, M. Bidy and A. Aden, *ACS 2010 Spring Meeting*, March 21-25, 2010, San Francisco CA.

“Thermodynamic analysis of fermentation and an aerobic growth of baker’s yeast for ethanol production,” K.-Y. Teh, A.E. Lutz, *Journal of Biotechnology* 147 (2010) 80-87.

“The role of thermochemical processing in optimizing the performance of future cellulosic ethanol biorefineries” C. Shaddix, E. Hecht, K.-W. Teh, A. Lutz, 3rd Annual World Congress of Industrial Biotechnology, July 25-27, 2010, Dalian, China.

“Combustion properties of biomass lignin residues” E.S. Hecht, C.R. Shaddix, 33rd International Combustion Symposium, Aug. 1-6, Beijing, China.

“Ionic liquid pretreatment with gel-free precipitation and IL recycling utilizing a phase-switchable solvent system,” Dean C. Dibble, Chenlin Li, Lan Sun, Anthe George, Aurelia Cheng, Özgül Persil Çetinkol, Peter Benke, Seema Singh, Blake A. Simmons, (2010) *in internal review prior to submission to Green Chemistry*.

“An Ionic liquid pretreatment process that includes IL recycling and a characterization of pretreatment fractions from corn stover” Dean C. Dibble, Chenlin Li, Lan Sun, Peter Benke, Anthe George, Seema Singh. Accepted for oral presentation at the AIChE Annual Meeting Nov. 7-12, Salt Lake City UT.

Several other journal papers are in preparation.

Appendix B

Arkenol Pretreatment Process Steps

1. prepare 77% sulfuric acid and cool overnight in refrigerator
2. slowly add 1.00 kg chopped biomass to 3.25 kg cool 77% sulfuric acid (giving 2.5:1 mass ratio of acid/biomass) in bioreactor
3. soak biomass in acid for 3 hours
4. add 4.10 L D.I. water to reactor
5. stir and heat reactor until reaches 99.5° C.
6. maintain at 99.5° C for one hour, while continuing to stir
7. remove from heat and pass liquids through a cloth filter
8. wash separated solids with 2 L D.I. water; repeat
9. dry solids in oven at 45° C
10. neutralize all collected liquids with mixture of 2.2 kg CaOH and 2.5 L D.I. water
11. filter out gypsum created in step 10
12. wash gypsum with D.I. water; repeat
13. dry gypsum
14. add dried solids to 77% sulfuric acid to make 2.5:1 mass ratio
15. repeat steps 3 – 13

